Numerical investigations on development of scramjet propulsion system

P.Nithish Reddy

A Thesis Submitted to
Indian Institute of Technology Hyderabad
In Partial Fulfillment of the Requirements for
The Degree of Master of Technology

भारतीय प्रौद्योगिकी संस्थान हैदराबाद
Indian Institute of Technology Hyderabad

Department of Mechanical Engineering

June 2013

Declaration

I declare that this written submission represents my ideas in my own words, and where ideas or words of others have been included, I have adequately cited and referenced the original sources. I also declare that I have adhered to all principles of academic honesty and integrity and have not misrepresented or fabricated or falsified any idea/data/fact/source in my submission. I understand that any violation of the above will be a cause for disciplinary action by the Institute and can also evoke penal action from the sources that have thus not been properly cited, or from whom proper permission has not been taken when needed.

P. Nithish Reddy

(Signature)

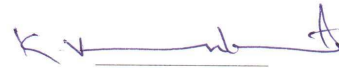(P.Nithish Reddy)

ME11M12

(Roll No.)

Approval Sheet

This Thesis entitled "Numerical investigations on development of scramjet propulsion system" by "P.Nithish Reddy" is approved for the degree of Master of Technology from IIT Hyderabad

(Dr. K.Arul Prakash) External examiner
Dept. of Applied Mechanics
IITM

(Dr. Raja Banerjee) Internal examiner
Dept. Mechanical Engg.
IITH

(Dr .K.Venkatasubbaiah) Adviser
Dept. Mechanical Engg.
IITH

(Dr. Narasimha Mangadoddy) Chairman
Dept. of Chemical Engg.
IITH

Acknowledgements

Dedicated to teachers who gifted me the knowledge

Abstract

In the present study various investigations are done on different components of scramjet propulsion system. In first part numerical investigations are carried out on transverse injection of fuel into the supersonic stream. Investigations includes the study of formation of recirculation regions , shock waves and wall pressure at different injection angles, free stream conditions and injection pressure ratio. Various turbulence models have been tested and the obtained results are well validated with the experimental. Formation of various structures due to sonic jet and supersonic stream interactions are analyzed. With increase in flow Mach number the size of auto ignition regions got minimized and jet injection angle shown the significant effect on the shock structure and peak pressure rise. Degree of boundary layer separation has increased with increase in pressure ratio. In the later part, investigations are done on DLR scramjet combustor where the fuel is injected parallel to the free stream using strut. Numerical investigation on flow phenomena in a scramjet combustor has been performed for different geometric and operating parameters. The present investigations aim to find the optimal geometric parameters and better fuel injection system which has maximum combustion efficiency. A combination of Eddy Dissipation (ED) and Finite Rate Chemistry (FRC) models are used to model the combustion. The effects of divergence angle on the performance of scramjet combustor are reported here. The effects of scaling on DLR combustor performance are reported. The effects of shocks created by strut and inlet conditions of scramjet combustor on combustion efficiency have been reported. A multiple struts combustor has been developed to improve the performance of combustor. Present results show that divergence angle and inlet conditions of combustor are significant on performance of scramjet combustor. Multiple struts combustor has shown higher efficiency than single strut combustor. In the final part the exit conditions of combustor used to evaluate the performance of scramjet nozzle. Numerical simulation of Single expansion ramp nozzle is carried out to investigate the effect of different geometric and operating conditions on performance parameters. Domain of investigation is chosen in such a way to capture the interaction between nozzle exit and hypersonic external flow. While evaluating the Thrust force both the internal and external surface of the ramp is taken in to consideration at various operating conditions. Based on this study, an optimum ramp angle at which the SERN generates maximum axial thrust is obtained for various operating conditions and behavior of the thrust and lift profile with various geometric changes at various operating conditions are predicted. Optimum angle for maximum thrust has shifted to left when simulated at higher operating conditions. Lower cowl angle, larger cowl and ramp length gave increased thrust and rate of increase varied from one operating condition to another.

Contents

List of Figures

Chapter 1

Introduction

In recent years aerospace technology development community is showing interest for hypersonic flight vehicles such as long-range passenger transport, reusable launch vehicles for space applications, and long-range missiles. Unlike turbojet or turbofan like jet engines, scramjet does not have rotating parts and need not to carry any oxygen cylinder like in rocket. Not only these advantages, but its capacity to achieve very high flight mach numbers placed scramjet in top priority in aerospace research.The successful development of such vehicles depends on the development of efficient propulsion system. From a cycle-efficiency viewpoint, the air-breathing engine is much superior than other chemical-propulsion engines because it uses oxygen from the air. Hypersonic air breathing propulsion system such as scramjet (Supersonic Combustion Ramjets) is one of the efficient propulsion systems for providing large thrust. Scramjet relies on high vehicle speed to compress and decelerate the incoming atmospheric air before combustion.

Scramjet propulsion system consist of three major parts: namely: (i) Inlet , (ii) combustor and (iii) Nozzle
1.An Inlet which compress the incoming air by shocks and feed to the combustor
2.A Combustor, where fuel reacts with compressed air and produces heat.
3.A diverging nozzle, where thrust force required to propel the vehicle is generated.

The flow field inside a scramjet combustor is highly complex. The mixing of reactants, flame holding, stability and complete combustion of fuel in shorter length are the major concerns in the development of scramjet engines.
For extracting maximum thrust from the expanding gases , an optimum nozzle has to be designed. A good nozzle should produce maximum thrust and should add less weight to the vehicle. Sern nozzle is one of the widely used nozzles in scramjet applications. Single expansion ramp nozzle, is a typical linear expansion nozzle. In this type of nozzle gas pressure transfers work only on one side. Unlike axially symmetric traditional nozzles Sern nozzle are not axially symmetric, but consist of two expansion ramps. Sern nozzle is widely

used because of its low weight at large expansion ratios. Also Sern produces additional lift at under-expansion.

The shape of the scramjet is designed in such a way that it generates significant amount of lift without any typical aero plane wing like structures. The lift generated from the other parts of the scramjet has to be balanced by nozzle and any imbalance will leads to pitching of the vehicle .Good control system is primary requirement when this type of nozzles are used. Recently in scramjet flight testing NASA used this nozzles in their hypersonic aircraft X-43 and was successful. The scramjet experiments are very complicated and only a few limited run times with affordable operating conditions are available. The most cost-effective way of investigating scramjet combustion therefore lies in the use of computational fluid dynamics (CFD), provided that the models have required fidelity. Present investigation has been focused on development of scramjet combustor using CFD.

The research on scramjet propulsion started with bell X-1 which attained supersonic flight in 1947.A variety of experimental scramjet engines are built and ground tested in US and UK laboratories. In 1964 Frederick S.Billing and Gordon L. Dugger submits a patent application for a supersonic combustion ramjet. An axisymmetric hydrogen fueled dual-mode scramjet was developed in late 1970s by Central institute of Aviation Motors (CIAM) . In 1981 tests were made in Australia under the guidance of Professor Ray Stalker in the T3 ground test facility at ANU. First successful flight test of Scramjet was performed by Russia in 1991. Then from 1992 to 1998 an additional 6 flight tests of the axisymmetric high-speed scramjet-demonstrator were conducted by CIAM together with France and then with NASA, USA. operated for 77 seconds, maximum flight speed of above Mach 6.4 is achieved. In the 2000s, research speeded up particularly with focus on improving scramjet engines. HYPER-X team[1] claimed the first flight of thrust producing scramjet powered vehicle with aerodynamic maneuvering surfaces named X-43A (Figure 1.1)in the year 2004. The HyShot came up with combustor project and successfully demonstrated it on July 30,2002.A series of scramjet ground tests supporting HIFiRE flight2 were conducted at NASA Langley Arc-Heated Scramjet Test Facility(AHSTF) at simulated Mach 8 flight conditions. HIFiRE (Hypersonic International Flight Research Experimentation) successfully tested a flight of hypersonic aircraft on May 22, 2009. In 2010 Australian and American defense Scientists tested a (HIFiRE) hypersonic rocket. It reached an atmospheric velocity of more than 5,000 kilometers per hour. On May 27,2010 ,NASA and United Air Force successfully flew the X-51A Waverider for approximately 200 seconds at Mach 5,setting a new world record in hypersonic air speed. Second test of X-51A Waverider at Mach6 was conducted on August 15, 2012 but it failed due to faulty control fin .

Figure 1.1: Artists Concept of the X-43a of NASP program

1.1 Scramjet component analysis

Figure 1.2 shows a schematic diagram of internal flow path in a scramjet vehicle. Station 0 is in the free stream flow ahead of the engine, and a stream tube with area A_0 is captured and processed by the engine. Station 1 is downstream of the vehicle fore body and represents the properties of the flow that enters the inlet. Station 2 is at the inlet throat, which is usually the minimum area of the flow path, and the length between stations 2 and 3 is referred to as the isolator. Station 3 represents the start of the combustor, and fuel and air is mixed and burned by the end of the combustor at station 4. The nozzle includes an internal expansion up to station 9, and an external expansion to station 10 at the end of the vehicle.
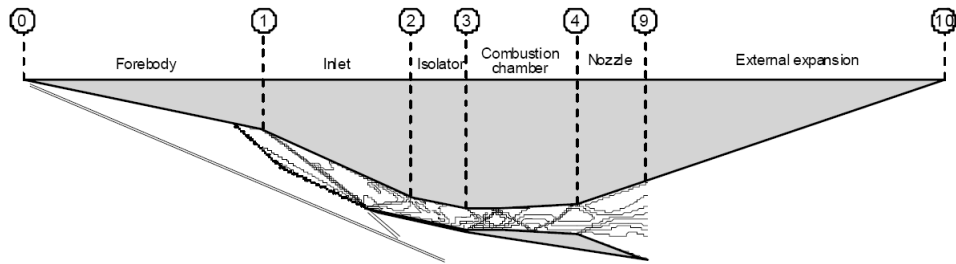
Figure 1.2: Flow stations of scramjet vehicle

1.1.1 Compression

For efficient combustion to take place, it is required that the air is supplied to the combustor at a suitable pressure, temperature and flow rate. For a scramjet, which operates at very high velocities and altitude, it is necessary to have significant compression and heating of the air before being processed into the combustion chamber. For an airframe integrated scramjet, both the vehicle fore body and the inlet share this task. Inlet consists of series of oblique shocks which compress the air as it passes through and at the same time turns the flow towards the combustion chamber.

1.1.2 Combustion

A combustor must contain and maintain stable combustion despite very high air flow rates. To do so combustors are carefully designed to first mix and ignite the air and fuel, and then mix in more air to complete the combustion process. Current research is facing following technical challenges in Engine Design.
Firstly the flow phenomena in Scramjet engine are very complex due to:
1. Shock shock interactions

2. Shock boundary layer, shock- shear layer interactions

3. Influence of shock waves on mixing and combustion efficiency

4. Turbulent mixing at supersonic speeds and heat release.

Thus it poses considerable challenge in design and development of a supersonic combustor with an optimized geometry. A good combustor must provide early ignition source, promote sufficient mixing of the air and fuel and flame holding regions so that the desired chemical reaction and thus heat release can occur within the residence time of the fuel air mixture. In order to accomplish this task, it requires a clear understanding of fuel injection processes and thorough knowledge of the processes governing supersonic mixing and combustion as well as the factors, which affects the losses within the combustor.

The designer shall keep in mind the following things to improve the Combustor performance,

Fuel injection system promoting

i) Good and rapid fuel air mixing

ii)Better Ignition and flame holding

iii) Operation over a range of inflow conditions.

Combustion in a scramjet engine can generate large pressure rise and separation of boundary layer on the surface of the combustion chamber. This separation, if it propagates into the inlet chamber can affect the compression process and may even unstart the engine. In order to avoid this, a short duct called as isolator is kept between the inlet and the combustion chamber to contain this phenomenon. Essentially, the purpose of the isolator is to stop the effects of the combustion from propagating upstream into the inlet.

1.1.3   Expansion

The expansion process converts the pressure energy of the combusting flow to kinetic energy and then thrust. In a scramjet, this begins in the divergent sections of the combustor and internal nozzle, and continues over a large portion of the vehicle after body. After body shape also determines the direction of net thrust of the scramjet vehicle.

A good nozzle should produce maximum thrust per its unit body weight and should operate efficiently at higher expansion ratios. SERN nozzle(Figure 1.3) is one of the widely used nozzles in hypersonic vehicles. Single expansion ramp nozzle, gives the advantage of extracting thrust from expanding gases and also creates the lift force.

  SERN Nozzle: Single expansion ramp nozzle, is a type expansion nozzle where the gas pressure transfers work only on one side. Unlike traditional nozzles, SERN nozzle is not have symmetric structure, they extract the thrust from its single ramp surface, see Figure 1.3. Thus this SERN nozzle gives the advantage of reduced weight and also the addition lift to propel the vehicle. As the gases expand along the ramp surface, thrust and lift forces are produced at a same time.
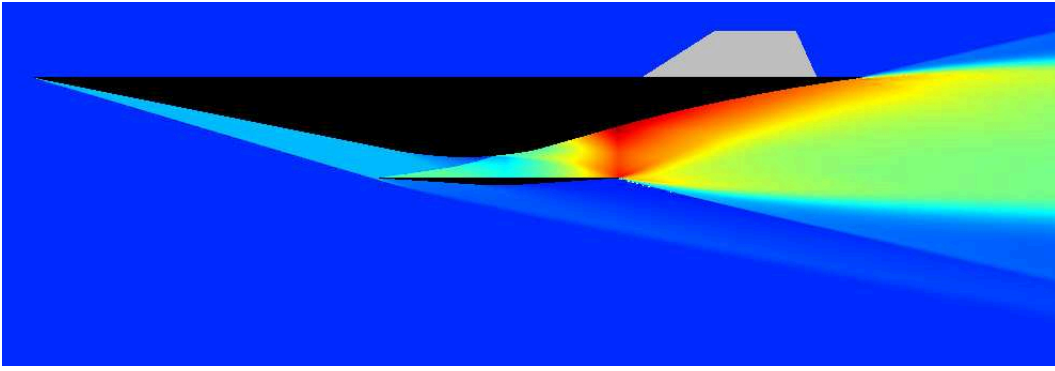
Figure 1.3: Scramjet with SERN nozzle

1.2 Fundamentals

Supersonic flow

Consider a body placed in a subsonic stream. As the flow interacts with the body several disturbances are created. These propagate at the speed of sound. Since the incoming flow is slower than sound, these disturbances can propagate upstream. As they propagate upstream, they modify the incoming flow. Consequently the flow adjusts itself to the presence of the body sufficiently upstream and flows past the body smoothly. This is also what happens with incompressible flows where the speed of sound is infinite.

  Figure 1.4 shows a body placed in flowing fluid. By interaction of fluid and object disturbances are created and these disturbances propagate at speed of sound. If the incoming flow is subsonic then the disturbances warns the incoming flow about the object ahead and thus the flow stream adjusts itself as shown in figure above. But if the incoming flow is supersonic then the speed of the flow is faster than the disturbance waves thus results in miscommunication .Due to this miscommunication the incoming flow doesnt notices the obstruction and thus results in sudden gradient in flow. In other words disturbances, unable to go upstream since the incoming flow is supersonic, are piled up closed to the body, see Figure 1.4. Now flow suddenly modifies itself to accommodate the presence of the body. This marks a sharp difference between subsonic and supersonic flows.

The example indicates that in a supersonic flow disturbances cannot propagate upstream. This technically stated asIn a Supersonic flows has no upstream influence. Further the region where the disturbances havepiled up is a Shock Wave. These are regions of infinitesimally small thickness across which flow properties such as pressure, density and temperature can jump, orders of magnitude, sometimes depending upon the Mach number of the flow. Consider an internal flow through duct of some cross sectional area. For subsonic , as the

6
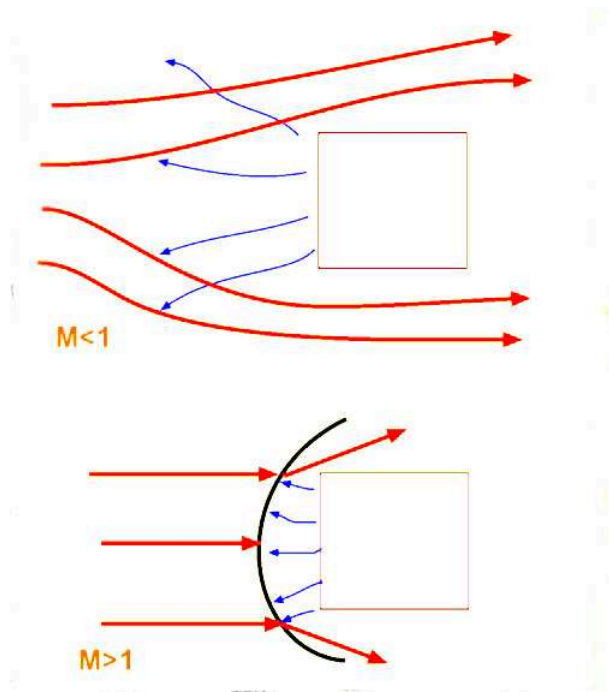
Figure 1.4: Comparison of sonic and supersonic flows

cross section area decreases velocity increases and vice versa. For supersonic flows, as the cross section area increases velocity increases and vice versa

This kind of behavior is due to the following reason:

At subsonic speeds as the cross sectional area is increased the velocity decreases (vice versa)and density changes are smaller. But in case of supersonic flows as the area increases density decrease at greater rate than velocity now the velocity increases to maintain the mass flow rate.

When Mach number of fluid is greater than 0.3 it is considered as compressible. So compressibility is the primary nature of all the supersonic flows. The behavior of fluid is variably different if its density is not constant. Numerically now we have to solve additionally equation of state to capture its behavior. In supersonic flow due to compressibility effects shock wave, expansion waves are formed.

1.2.1   Shock wave

A shock wave is a type of propagating disturbance commonly observed in supersonic($1 < M < 5$) and hypersonic flows($M > 5$).Generally they form due to presence of wedge, concave corners in a case of external flows and due to overexpansion in internal flows.

Shock waves are of two types :

i. Oblique shock

ii. Normal shock

i)Oblique shock waves:

Oblique shocks are the straight compression shocks inclined at an angle to the upstream flow direction. Across the oblique shock the velocity of the flow falls down and rest of the properties like temperature, pressure, density increases. Also the flow direction chances when oblique shockwave is en countered as shown in figure 1.5.

The angle at which this oblique shock wave inclined depends upon the flow Mach number,
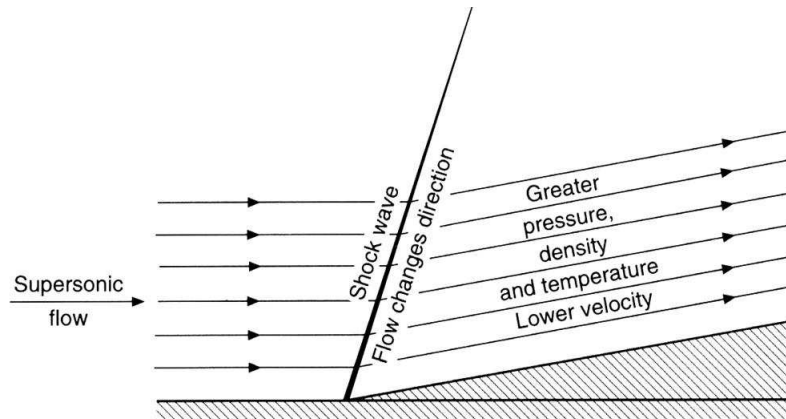
Figure 1.5: Oblique shock

kind of obstacle. Figure 1.6 shows the formation oblique shock wave inclined at an angle by the presence of wedge having an angle when the Mach number of the upstream fluid is M.

ii) Normal shock: This shock wave is straight with the flow at right angles to the wave.
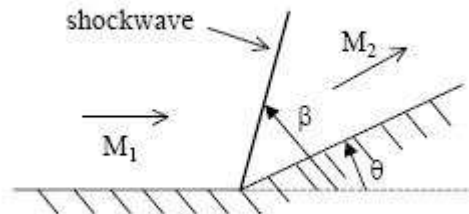
Figure 1.6: Defelction angle

Shockwaves are established in supersonic flow as a solution to the problem of disturbance propagating through a flow. Formation of shock wave results in change of flow from supersonic to subsonic.

Figure 1.7 shows the property change across the normal shock wave. The arrows in the figure indicate the flow direction. Across the pressure, temperature, density, entropy
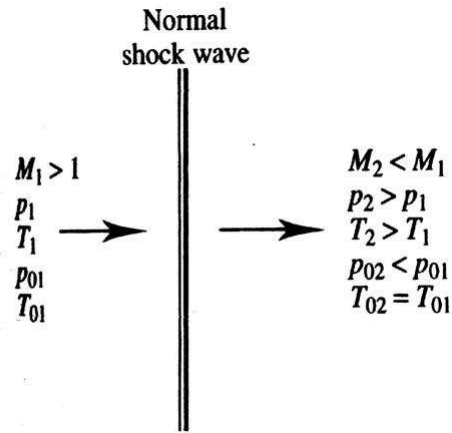
Figure 1.7: Normal shock

increase and total pressure and total temperature decreases

1.2.2 Expansion wave

Expansion waves are formed when flow is allowed to deflect freely where as in case of shock waves an obstacle forcefully deflects the flow. Unlike shock waves expansion waves are not sharp, the flow properties varies gradually forming an expansion fan. Across the expansion wave pressure, temperature, density of the flow decreases where as the velocity of the flow increases.
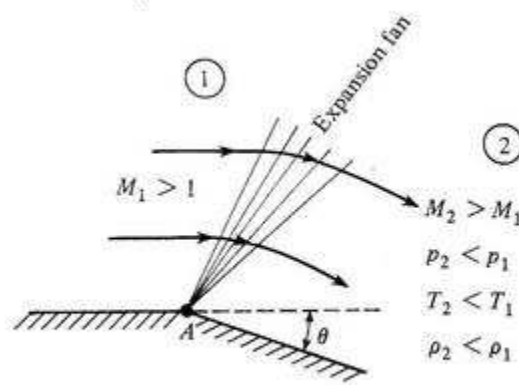
Figure 1.8: Expansion wave

1.2.3   Flow Phenomena

Generally in compressible flows most commonly observes flow phenomenas are shock reflections, shock shock interaction, shock boundary layer interaction. These phenomenas are fore most important to study to get full picture of effects of varying density.

i)Shock reflections:

When a shock wave incidence a surface it gets reflected back at some angle .The angle of reflection and the properties across such reflected shock wave varies depending number of factors.

  Properties across the shock depends upon the properties of flow before incidence and de-
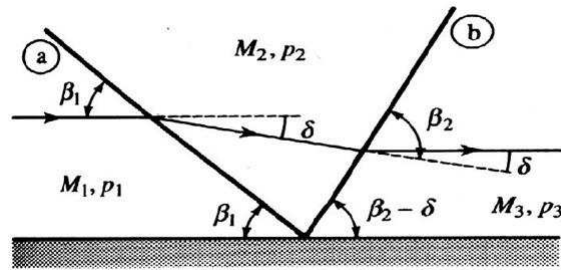
Figure 1.9: Shock reflecting from surface

flection angle.

ii)Shock shock interactions:

Majorly in case of internal flows and sometimes in case of the external flow the phenomena of shock-shock interactions are observed.
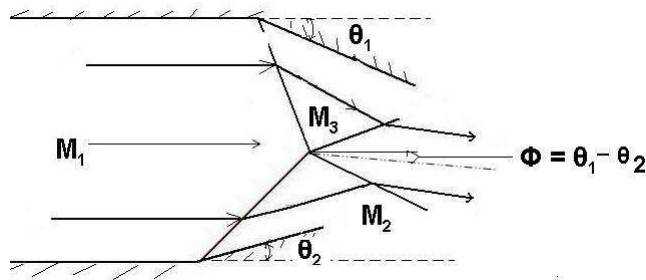
Figure 1.10: Shock-shock interactions

    Figure 1.10 shows the resultant flow direction when two shock waves interacts. Flow property changes across the shock waves changes similar way as discusses in the section of oblique shock waves. The dotted line in the figure shown is called slip line.

iii)Shock- boundary layer interactions:

Shock Wave/Boundary Layer Interaction (SBLI) is a fundamental phenomenon in gas dynamics and frequently a defining feature in high speed aerodynamic flow fields. The in-

teractions can be found in practical situations, ranging from transonic aircraft wings to hypersonic vehicles and engines. SBLI's have the potential to pose serious problems and is thus a critical issue for aerospace applications. This phenomena is fore most important to analyze in supersonic flows since any abrupt changes in the boundary layer disturbs the entire flow.
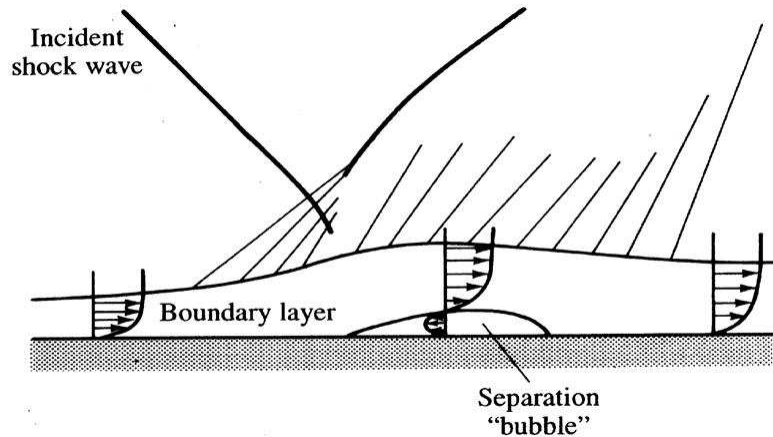
Figure 1.11: Shock-boundary layer interactions

The shock produces an adverse pressure gradient along the boundary layer, which causes the flow to slow and the boundary layer to thicken. In the limit the flow may recirculate, and the boundary layer will detach from the wall.

Figure 1.11 shows the graphical view of velocity profile in boundary layer and its changes due to shock impingement. In the separation bubble the direction of flow has changed and velocity profile with negative velocity is noticed

Fuel injection

Among fuel used for jet propulsions hydrogen serves better for scramjet. Jacobsen et.al.[2] reported that hydrocarbons present more of a challenge compared to hydrogen due to the longer ignition delay and the requirement for more advanced mixing techniques. The objective is to achieve better mixing in shorter length which has to be considered in designing the combustor. There are several other key issues that must be considered in the design of an efficient fuel injector. As already discussed an efficient injector should also provide a source for ignition and local region suitable for flame holding. A good injection process should support rapid mixing and combustion of the fuel and air with minimized losses .It is always advantageous to have best suited injection system because it reduces the length of combustor and there by weight of combustor. There are two primary ways to inject fuel

11

in to scramjet:

A. Transverse injection/normal in to main flow

B. Parallel injection

At lower flight Mach numbers (below Mach 10) we can use normal injection but at higher Mach number parallel injection in to inlet air stream since the fuel momentum provides a significant portion of the engine thrust.

1.2.4   Transverse injection

One of the simplest approaches is the transverse (normal) injection of fuel from a wall orifice .This type of injection is simple in construction and creates complex flow behavior.
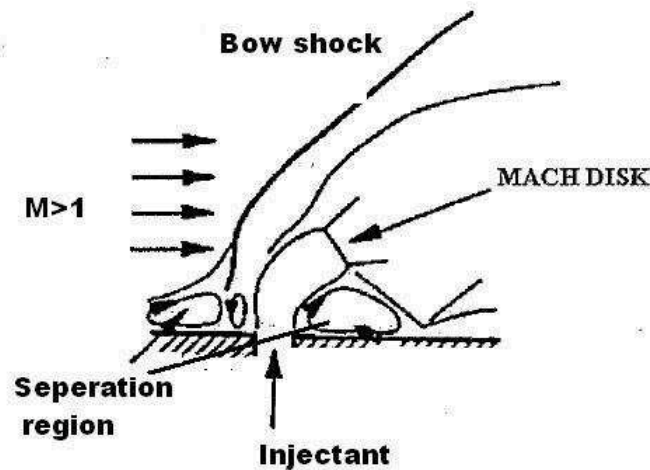
Figure 1.12: Injectant jet and cross flow interaction

Figure 1.12 shows schematic diagram of interaction of sonic jet with cross flow. When a jet is introduced or injected normally in to a supersonic stream ,a bow shock is produced upstream of the jet exit. Huber et.al.[3, 4] reported that this shock formation separates the upstream wall boundary layer providing a region where the boundary layer and jet fluids mix sub sonically. This region is important in transverse injection flow fields because of its flame-holding capability in combusting situations. However, this injection configuration has stagnation pressure losses due to the strong three-dimensional bow shock formed by the normal jet penetration, particularly at high flight velocities.

The major drawback of this injection system is low jet penetration. We use number of such wall injectors simultaneously with proper placement to achieve required amount mixing. There are also other techniques to improve the fuel air mixing. One of them is to use some convoluted surfaces on walls of combustor near injector. Introduction of tabs or some wedge shaped bodies on the wall of combustor creates vortices in flow field. Addition of vortices

to the flow creates good environment for fuel-air mixing.

1.2.5 Parallel Injection:
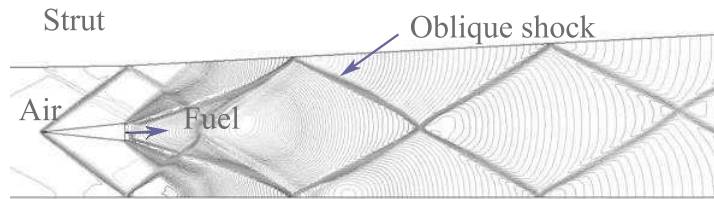
Figure 1.13: Strut injection

Figure 1.13 shows the central strut injection system. Strut based injector is used to inject fuel parallel to air stream. This injector is commonly placed in the centre of the combustor. It gives the advantage of injecting fuel in to the core of the air stream. The base of the strut serves as flame holder by creating wake behind it . Another advantage is the oblique shocks produced from the leading edge of the strut enhance the mixing of air and fuel.

1.3   Literature survey

1.3.1   Fuel injection:

Transverse injection in to supersonic flow is one of the important phenomena to study as it has several applications like fuel injection in scramjet combustors and in other space vehicles. A blow shock forms ahead of the jet which pressure gradient in boundary layer , resulting in a separation bubble. Figure 1.12 shows schematic diagram of interaction of sonic jet with cross flow. This Figure shows one recirculation region one upstream of the jet and another downstream of the jet orifice. Also a Mach disc is observed in Figure which is due to the highly under expanded jet as said by Baurle et. al.[5].

Behavior of the vortical structures involved in transverse injection ,specially focusing on low speed flows was reported in Fric et.al.[6].The results revealed the formation of 4 coherent structures .One vortex wrapping around the jet, second in downstream wake, third near field jet-shear layer vortex, forth far field counter rotating vortex pair. After realizing the importance of these stream wise counter-rotating vortices many researches concentrated on different injection strategies focusing on generation of these structures[7, 8, 9]. Riggens et al. [10] study of angle injection at high flight mach number gave good results .At mach 13.5 and Mach 17 flight mach number by injection fuel at 30 deg thrust has improved .It is concluded that the fuel jet momentum added to the net thrust potential by such angled injection in to high speed flows. Later part of the research concentrated on the influence of different fuel on formation of these structures and jet penetration. The conclusions were the molecular weight of fuel shown big variation in injection velocities which influences jet shear layer growth rate and the mixing properties. Studies focusing on the jet penetration revealed that molecular weight of the fuel have no much effect on the jet penetration [11, 12, 13, 14, 15]. However, efficient fuel-air mixing, jet penetration does not directly initiate the combustion process, Ignition and flame holding also plays major role. A Study of auto ignition of hydrogen jet injected transversely into hypersonic flow predicated that upstream recirculation region of the jet and behind the bow shock are found to be sources of ignition[16, 17]. Kyung et.al.[18]numerical investigated on combustion enhancement when a cavity is used for the hydrogen fuel injection through a transverse slot nozzle into a supersonic hot air stream. Wei Huang etal. [20] reported the influences of the turbulence model and the slot width on the transverse slot injection . Kim et al.[19] numerically validated the experimental results of transvese injection into supersonic stream.

1.3.2   Combustion:

One of the first attempts in addition of heat to a supersonic flow gas in a constant area duct was done by Foa et.al.[21]. Later Stocker[22] discussed the transient effects arising from the addition of heat to supersonic flow of gas in a pipe. A comprehensive review on mixing controlled supersonic combustion was given by Antonio Ferri et.al.[23]. Heiser and Pratt

et.al.[24] provided an overview on the concepts of fuel-air mixing and mixing controlled supersonic combustion. A comprehensive review on scramjet propulsion was reported by Curran et.al.[25]. Seiner et.al.[26] made a survey on different injection systems like cavity, wall injection and central injection used in scramjet engines. Rowan et.al.[27] experimentally studied the effects of combined tangential and normal fuel injection in scramjet combustor and found best performance with complete normal injection. Comprehensive review on supersonic combustion with cavity based fuel injection were reported[28, 29]. Mathur *et.al.*[30] performed experimental study on supersonic combustion with a cavity based fuel injector and demonstrated successful ignition, sustained combustion of gaseous ethylene. The oblique shocks generated from strut augment the fuel-air mixing for central strut injection system. Kim et.al.[31] numerically studied such mixing enhancement by shock waves in scramjet engines. Numerical study on the effects of transverse jet injection into a supersonic turbulent flow in scramjet combustor was done by Rana *et.al.*[32]. They found that Kelvin-Helmholtz type instabilities in the upper jet shear layer are primarily responsible for mixing of the two fluids.

One of the pioneer experimental results on scramjet combustion with hydrogen fuel in a simple geometry at the Institute for Chemical Propulsion of German Aerospace Center, DLR reported by Waidmann *et.al.*[33, 34, 35] and these results were considered as reference in the literature for the development of Computational Fluid Dynamics (CFD) model on scramjet engines. Numerical investigation of turbulent hydrogen combustion in a scramjet using flamelet model was done by Oevermann*et.al.*[36]. He has used -probability density function to describe the coupling between turbulence and non-equilibrium chemistry of the flame. Berglund *et.al.*[37]performed large eddy simulation (LES) on supersonic flow and combustion in a DLR scramjet combustor .They have performed simulations for non-reacting and reacting flow fields in scramjet combustor. The effects of chemistry models on supersonic combustion of hydrogen was numerically investigated by Kumaran and Babu*et.al.*[38]. They reported that multi step chemistry model shown a higher heat release both in mixing controlled and kinetically controlled regions than a single step chemistry model. Dharavath *et.al.*[39] numerically studied the thermo chemical exploration of hydrogen combustion in scramjet combustor. Shock wave/boundary layer interactions is one of the important aspect has to be considered in design of supersonic combustor. The presence of turbulent separation can result in large fluctuating pressure loads and high heat transfer rates, and can cause damage or rapid fatigue of aero-structures. Experimentally investigated the phenomena of shock wave/turbulent boundary layer interactions and shock induced separation was done by Dussage *et.al.*[40]. They found that the frequency of fluctuations produced by the shock motion is much lower than the characteristic frequencies of turbulence in the incoming boundary layers. Ganapathisubramani *et.al.*[41]studied the effects of upstream boundary layer on the unsteadiness of shock-induced separation. Humble [42] experimental study on the instantaneous 3D flow organization of a shock wave/turbulent boundary

15

layer interaction using tomographic particle image velocimetry. A comprehensive review on numerical simulations of shock/boundary layer interactions was reported by Edwards et.al.[43]. The inlet of scramjet engine must be designed to improve the compression process and also deliver supersonic air to the combustion chamber. The approach of Bilevel Integrated System Synthesis (BLISS) method was used for optimization of scramjet inlet and flow phenomena in three subsystems of scramjet: inlet, combustor and nozzle were studied using CFD by XuDajun et.al.[44]. Optimization was done using one dimensional gas dynamic relations. Recently a new approach for design of scramjet inlets was done by Prakash and Venkatasubbaiah [45]. They have used the gas dynamic relations to optimize the inlet geometry and analyzed the flow phenomena in scramjet inlet using CFD.

1.3.3 Expansion:

Supersonic thrust nozzles are essentially used to make the flow to accelerate through it and extracts thrust out of it. SERN is also one of such thrust nozzles. This single expansion ramp nozzle (SERN) gives an advantage of reduced weight while extracting most of the thrust from the high-pressure flow on the after body [46]. Because of this special characteristics of thrust to weight ratio this type of nozzles drawn the attention of many researchers. Lederer *et.al.*[47] stated the importance of developing efficient nozzle in producing trust considering weight constraint into account. Stephen *et.al.*[52] numerically simulated hypersonic flow through Sern in early 1992. Hirschen *et.al.*[53] studied the aerodynamic phenomena and their effects on the nozzle performance. In his study Christian *et.al.*[54] used pressure sensitive paint which gives detailed pressure information on whole surface. Monta *et.al.*[55] did experimental study on single expansion ramp nozzle which is taken as bench mark problem for validation of code.

In later part of research many people did different parametric studies which include: Hirrman et.al [56] studied the influence of heat capacity ratio on nozzle flow field. Li et.al.[57] studied the effect of different parameters on designed nozzle performance using a solver. Thiagarajan *et.al.*[58] studied the effect of side fence and other parameters on nozzle performance. Hirschen *et.al.*[59] studied the aerodynamic phenomena and their effects on the nozzle performance. Tetsuo *et.al.*[60] studied the performance of scramjet nozzle at various nozzle pressure ratios. An overview for research on engine/airframe integration for hypersonic vehicles is given by Huang *et.al.*[61]. Role of chemically reacting flow of fuel and air on nozzle performance is studied by Sangiovanni, *et.al.*[62]. Lee *et.al.*[63] studied the reactive flow field in scramjet nozzle. Wei Huang *et.al.*[64] proposed a efficient method in designing and optimizing the nozzle configuration.

1.4   Motivation

In the literature detailed ground base information about scramjet combustor design and proper understanding of flow physics involved in formation of different shock patterns in combustor and importance of divergence angle of combustor are not clearly shown. This has been the motivation for present investigation. Most of the experimental work is done with affordable operating conditions and it is also expensive to do number of parametric investigations in supersonic experiments. The optimum geometric parameters vary from the one environment to another. In literature numbers of studies are done but evaluation of lift and drag forces considering both internal and external flow field is rare. Performance characteristics at different flight Mach numbers with corresponding nozzle inflow conditions are also rarely available. To study the behavior of thrust profile at high operating conditions experimentally is very difficult and requires test facility which with stands force involved. Also only few limited runs are available thus CFD became an alternative way to conduct the investigations at practical flight worthy operating conditions.

1.5   Objective of current study

The objective of the current study is to investigate the effect of various parameters in design and development of scramjet combustion and expansion system. Present investigations aims at understanding the flow behavior in different components of scramjet propulsion system at different conditions and optimize parameters for better performance. The problem statement(s) of the current study is summarized as follows:

- To study the significance of the divergence angle in combustor design.

- To study the formation of different shock structures and their influence on performance.

- To study the combustor flow field at operating conditions close to real fight environment.

- To study the complete nozzle flow field for different combustor exit conditions.

- To present the significance of geometric parameters and operating conditions on nozzle performance.

- To know influence of various injection configurations and flow conditions on interaction between jet and cross flow.

1.6   Outline of thesis

Chapter 1 gives the preliminary fundamental study about scramjet and present challenges in this area of research. This chapter presents the motivation and objective behind choosing this problem.

In chapter 2 numerical methodology used for a given physical problem is presented. This chapter gives details of physical model, governing equations being solved and numerical models adopted. The underlying basic information of turbulence model and functioning of combustion modeling is presented. In chapter 3 presents the pre-processing work and results of transverse injection system . Firstly computational grid for physical domain and the dependency of solution for different grid is presented. In later section predicted numerical results are compared with experimental results. In the final part results obtained in various studies are documented.

In chapter 4 results obtained for the combustor is analyzed. Present results are validated with the experimental .The effect of different parameters are discussed.

In chapter 5 results are discussed for nozzle flow field are presented. In first section shows grid independence study,validation then effect of different geometric parameters are analyzed and in following section performance characteristics at various operating conditions are evaluated. In Chapter 6 conclusions of the current work is presented systematically. Chapter 7 gives some inputs for further investigations.

Chapter 2

Formulation and Numerical methods

2.1 Physical model

2.1.1 Fuel injection

Figure 2.1 shows a schematic diagram of wall injection system. This problem of injection flow is considered following the experimental configuration and flow conditions of Aso et al.[66]. The geometry consists of a flat with a slot. The distance of slot from the leading edge is L =330 mm. The calculation is conducted for free stream Mach number of 3.75, total pressure of 1.2 MPa, and total temperature of 299 K. A slot nozzle is convergent sonic throat at the exit. Nozzle width is 1.0 mm while nitrogen gas is injected with pressure ratio(P) of 10.29. The injection total pressure to free stream pressure ratio is defined as pressure ratio.

Air M_∞

$L_{ref} = 330\,mm$ 1mm

θ

N2

$L/L_{ref} = 1.3$
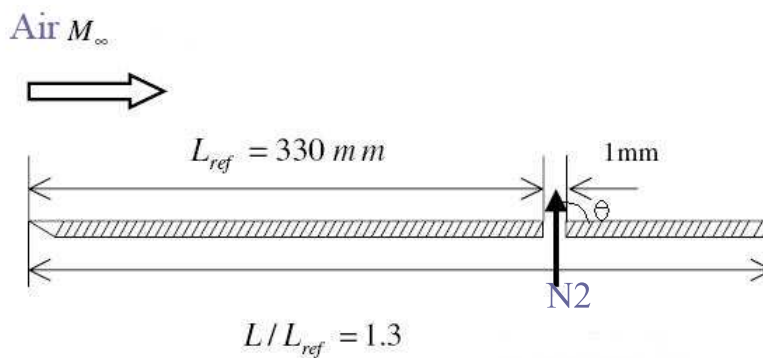
Figure 2.1: Geometry

2.1.2 Combustor

Figure 2.2 shows a schematic diagram of scramjet combustor used by Waidmann et al[33, 34, 35] at the Institute for Chemical Propulsion of German Aerospace Center, DLR. Air is preheated by the combustion of hydrogen in a heater and it is expanded through a Laval nozzle. From Laval nozzle air enters the combustion chamber at M = 2.0. The combustor has a width of 40 mm and a height of 50 mm at the entrance, 62 mm at the exit. A divergence angle of 3 degrees is provided at the upper wall after a certain distance from inlet as shown in Figure 2.2. A wedge shaped strut having half wedge angle of 6 degrees and 0.032 m long is placed at mid plane at a distance of 77 mm from inlet. Strut has 15 holes with diameter of 1 mm each are used for injecting hydrogen fuel parallel to the air stream at sonic conditions. These injection holes are placed 0.0028 m apart from each other.
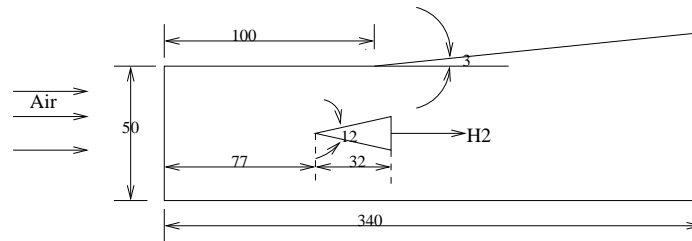
Figure 2.2: Schematic diagram of central strut combustor.

2.1.3 Nozzle

For the investigation a model is taken from the experimental work of Monta et al.[55] at NASA. SERN (Single expansion ramp nozzle)with ramp angle 20 deg,cowl angle 12 deg to validate the code. The physics domain is chosen to analyze the flow both internal and external to nozzle as shown in the computational grid(Figure 2.3).Other dimensions of the nozzle include ,cowl height of 0.417h , the horizontal length of the inner nozzle(s) is1.7h, where h=15.24 mm. The length of the whole nozzle is chosen as 20h as shown in Figure 2.3. In Experimental study Monta *et.al.*[46] used pitot tube set to measures the pressure distribution at various points along different section. In applying pitot pressure measurements in supersonic and hypersonic flow regimes, a normal shock wave occurs in front of the pitot tube so numerical results are validated with experimental considering shock effect as done by Wei Huang *et.al.*[64].
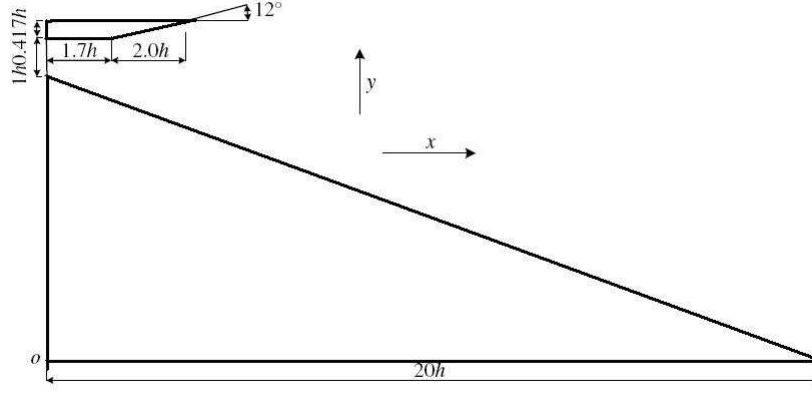
Figure 2.3: Schematic diagram of single expansion ramp nozzle with 20 deg ramp angle (1h=15.24 mm).

2.2 Governing equations

Flow field is governed by the following fundamental equations: i)Continuity equation:

$$\frac{\partial \rho}{\partial t} + \frac{\partial}{\partial x_j}[\rho u_j] = 0, \quad j = 1, 2, 3 \tag{2.1}$$

ii)Momentum equations:

$$\frac{\partial}{\partial t}(\rho u_i) + \frac{\partial}{\partial x_j}[\rho u_i u_j + p\delta_{ij} - \tau_{ji}] = 0, \quad i, j = 1, 2, 3 \tag{2.2}$$

iii)Energy equation:

$$\frac{\partial}{\partial t}(\rho e_0) + \frac{\partial}{\partial x_j}[\rho u_j e_0 + u_j p + q_j - u_i \tau_{ij}] = 0, \quad i, j = 1, 2, 3 \tag{2.3}$$

Where

$$\tau_{ij} = \tau_{laminar} - \tau_{turbulent} \tag{2.4}$$

$$\tau_{laminar} = \mu \left(\frac{\partial u_i}{\partial x_j} + \frac{\partial u_j}{\partial x_i} \right) \tag{2.5}$$

$$\tau_{turbulent} = \rho u_i' u_j' \tag{2.6}$$

Along with the above three equations chemical species transport equations are to be

21

solved for reacting flows.

2.2.1 Turbulence modeling

It computationally very expensive to resolve the complex flows. Fluent code facilitates efficient turbulent models to predict the flow filed without undergoing the trouble of resolving. One of most popular turbulent model in use is two equation $k - \epsilon$ turbulent models. It is a two equation model, that means, it includes two extra transport equations to represent the turbulent properties of the flow.

Turbulent kinetic energy- k, dissipation rate- ϵ are the two transport variables. Turbulent dissipation rate determines the scale of the turbulence. Energy in turbulence is determined by k.

$k - \epsilon$ model has been shown to be useful by Bardina et.al.[65] for free-shear layer flows with relatively small pressure gradients. Similarly, for wall-bounded and internal flows, the model gives good results only in cases where mean pressure gradients are small; accuracy has been shown experimentally to be reduced for flows containing large adverse pressure gradients. One might infer then, that the $k - \epsilon$ model would be an inappropriate choice for problems such as inlets and compressors.

Transport equations for $k - \epsilon$ model :

Turbulent kinetic energy equation:

$$\frac{\partial}{\partial t}(\rho k) + \frac{\partial}{\partial x_i}(\rho k u_i) = \frac{\partial}{\partial x_j}\left[\left(\mu + \frac{\mu_t}{\sigma_k}\right)\frac{\partial k}{\partial x_j}\right] + P_k - \rho\epsilon \tag{2.7}$$

Turbulent dissipation rate equation:

$$\frac{\partial}{\partial t}(\rho \epsilon) + \frac{\partial}{\partial x_i}(\rho \epsilon u_i) = \frac{\partial}{\partial x_j}\left[\left(\mu + \frac{\mu_t}{\sigma_\epsilon}\right)\frac{\partial \epsilon}{\partial x_j}\right] + C_{1\epsilon}\frac{\epsilon}{k}P_k - C_{2\epsilon}^*\rho\frac{\epsilon^2}{k} \tag{2.8}$$

Where

$$C_{2\epsilon}^* = C_{2\epsilon} + \frac{C_\mu \eta^3(1-\eta/\eta_0)}{1+\beta\eta^3}$$
$$\text{And } \eta = Sk/\epsilon \ , \ S = (2S_{ij}S_{ij})^{1/2}$$

Turbulent viscosity is given by,

$$\mu_t = \rho C_\mu \frac{k^2}{\epsilon} \tag{2.9}$$

And the corresponding constants are:

Constants

$$C_\mu = 0.0845$$
$$\sigma_k = 0.7194$$
$$\sigma_\epsilon = 0.7194$$
$$C_{\epsilon 1} = 1.42$$
$$C_{\epsilon 2} = 1.68$$
$$\eta_0 = 4.38$$

2.2.2 Combustion modeling

For the combined Finite Rate Chemistry/Eddy Dissipation Model, the reaction rates are first computed for each model separately and then the minimum of the two is used. This procedure is applied for each reaction step separately, so while the rate for one step may be limited by the chemical kinetics, some other step might be limited by turbulent mixing at the same time and physical location.

The combined model is valid for a wide range of configurations, provided the flow is turbulent. In particular, the model is valid for many reactions that range from low to high Damkhler numbers (chemistry slow/fast compared to turbulent time scale). Use of this model is recommended if reaction rates are limited by turbulent mixing in one area of the domain and limited by kinetics somewhere else. The Eddy Dissipation model can, however, be more robust than Finite Rate Chemistry or the combined model [48].

Eddy Dissipation is used to model one- or two-step global (heat release) reaction mechanisms. Solves species transport equations. Reaction rate is controlled by turbulent Mixing. The rate of reaction is then determined from the minimum of the mixing and kinetic net rate and is expressed as $K_r = \min(K_r,\text{edm}, K_r,\text{frc})$

A rate law is an equation that tells us how fast the reaction proceeds and how the reaction rate depends on the concentrations of the chemical species involved.

In finite rate chemistry model Arrhenius equation is used to determine the rate of reaction . The forward rate constant for reaction r ,K_r , is computed using the Arrhenius expression:
$K_r = AT^B e^{(-E/RT)}$

The values of A,B E are taken as A=8.99e+08 , E=2.9e+07 , B=0 .

where: A = pre-exponential factor (consistent units) B = temperature exponent (dimensionless) E= activation energy for the reaction (J/kmol)

The Eddy Dissipation model is best applied to turbulent flows when the chemical reaction rate is fast relative to the transport processes in the flow. There is no kinetic control of the reaction process. Chemical reaction rate is governed by the large-eddy mixing time scale,

k/ϵ, as in the eddy-breakup model of Spalding [72]. Combustion proceeds whenever turbulence is present ($k/\epsilon > 0$), and an ignition source is not required to initiate combustion. FLUENT allows multi-step reaction mechanisms (number of reactions > 2) with the eddy-dissipation and finite-rate/eddy-dissipation models, these will likely produce incorrect solutions. The reason is that multi-step chemical mechanisms are based on Arrhenius rates, which differ for each reaction. In the eddy-dissipation model, every reaction has the same, turbulent rate, and therefore the model should be used only for one-step (reactant → product), or two-step (reactant → intermediate, intermediate → product) global reactions.
In practice, the Arrhenius rate acts as a kinetic "$switch''$", preventing reaction before the flame holder. Once the flame is ignited, the eddy-dissipation rate is generally smaller than the Arrhenius rate, and reactions are mixing-limited.

2.3 Numerical method

Numerical code of commercial CFD solver Fluent is used to carry out the current investigation. Fluid is taken as air with ideal gas assumption and flow is modeled with second order accurate schemes . Double precision calculations are done to avoid the growth of round of error. Proper under relaxation factor are chosen and the courant number is set as 0.05.Two-equation $RNGk - \epsilon$ turbulent model is used to model turbulence. Ferguson et.al.[73] reported that $RNGk - \epsilon$ turbulent model with non equilibrium wall functions proven to be good in model flow near walls. The RNG model was developed using Re-Normalization Group (RNG) methods to account for the effects of smaller scales of motion. Because of the capability to partly account for the effects of pressure gradients, the non-equilibrium wall functions are recommended for use in complex flows involving separation, reattachment, and impingement where the mean flow and turbulence are subjected to pressure gradients and rapid changes. In such flows, improvements can be obtained, particularly in the prediction of wall shear (skin-friction coefficient) and heat transfer (Nusselt or Stanton number). In order to simulate the combustion the Navier-Stokes equations must be complemented with a chemical reaction mechanism and a thermodynamic model. The chemical reaction mechanism prescribes how fuel and oxidant react, what products are formed and their mutual relations. The thermodynamic model describes how much energy is dissipated. Air is considered as an ideal gas with variable properties. Combustion is modeled using a combination of finite rate chemistry (FRC) model and eddy dissipation (ED) model. The finite rate chemistry model along with eddy dissipation model avoids the expensive Arrhenius calculations where reaction rates are controlled by turbulence. The following single step reversible reaction has been chosen.
$2H_2 + O_2 \rightarrow 2H_2O$
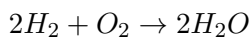
2.3.1 Boundary conditions

No-slip boundary conditions are imposed at the solid walls for velocity field. Adiabatic boundary condition is used at the solid walls for temperature field. Appropriate flow variables are specified at inflow and flow variables at outflow are extrapolated from the interior. Since the flow is supersonic throughout the domain the information passes only in forward direction and thus outflow now becomes zone of concern rather than zone of dependence.

Chapter 3

Results and discussion on Fuel-injection

3.1 Grid independence study

Required computational grid for the transverse injection analysis is generated using Ansys ICEM CFD . Grid is made finer near the injector and at walls to capture the jet and shock/boundary layer interactions. Wall Y^+ is maintained less than 5 near wall. Numerical simulations are obtained with three different grid sizes: coarse mesh 8000 cells, medium mesh 15000 cells, and fine mesh 25000 cells. The length of the upstream separation region and other parameters are predicted well by all grid scales. In Figure 3.1, the numerically
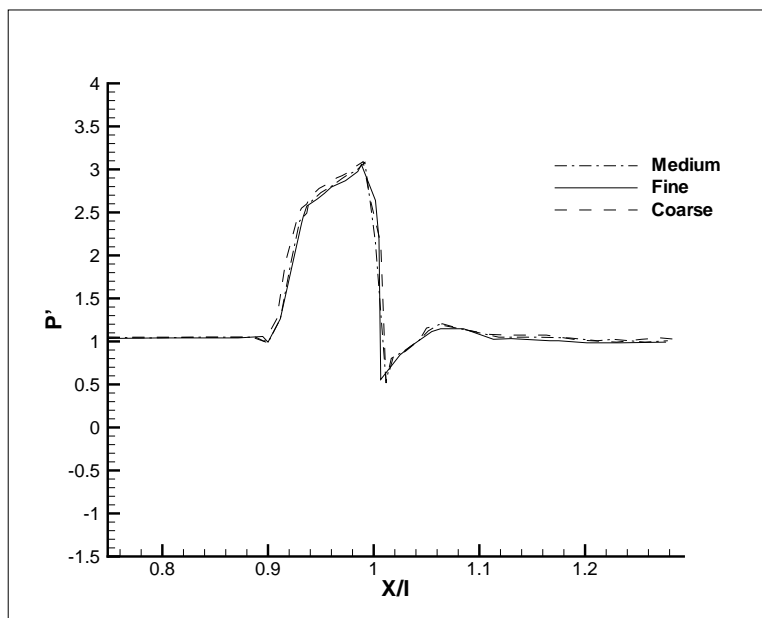

Figure 3.1: Comparision of wall pressure for different grids

predicated wall pressure for different grid sizes are plotted . It is found that there is not much variation in results with grid size. Thus coarse mesh is used in our investigation.

3.2 Validation

Numerically predicated results are compared with the experimental data by Aso et al. [66].The experimental free stream Mach number of 3.75, total pressure of 1.2 MPa, and total temperature of 299 K are taken at inflow. Nitrogen gas is injected with pressure ratio(P) of 10.29 at sonic conditions from a slot of width 1.0mm.
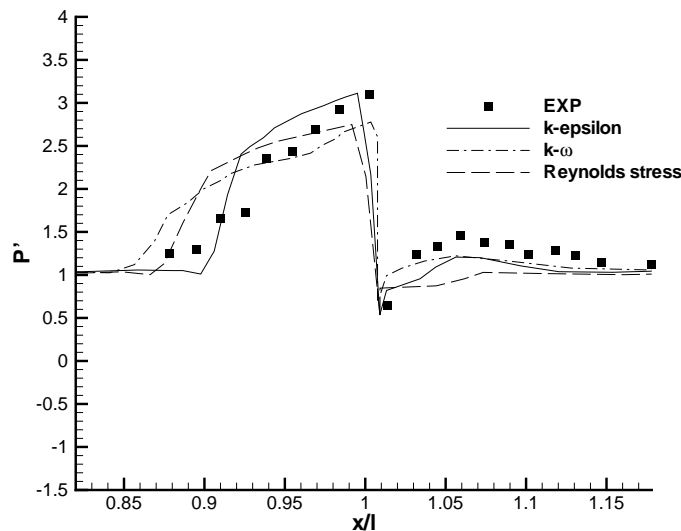
Figure 3.2: Comparison of predicted wall pressure with experimental results

In Figure 3.2, the numerically predicated wall pressure is plotted and compared with the experimental data by Aso et al. [66]. Current results shown reasonable accuracy with other numerical results, some discrepancy is observed when compared with experimental data. The discrepancy may be because the experiment do not record sharp peak just upstream of the injection slot and there are limitations in pressure probes placement in case of supersonic flows.

Numerical results obtained by the $RNGK\epsilon$ turbulence model show better agreement with the experimental data than the other turbulence models, namely the Reynolds stress and $K - \omega$ turbulence models. At the same time, the length of the upstream separation region and the peak pressure upstream of the injection slot are under estimated by Reynolds stress model and the $k - \omega$ turbulence model. The recirculation zone plays a significant role in chemically reacting flows [67]. In this region, the velocity is low, and the flames can be sustained [68]. Thus it is important to capture the upstream recirculation zone . RNG $k - \epsilon$

model is able to predict the length of the upstream recirculation zone, thus this model is used for the rest of the investigations.

3.3   Transverse jet and supersonic flow interactions

In the current study, free stream parameters temperature and pressure are chosen as 340k and 1bar respectively throughout the investigations and the corresponding total pressure and total temperature at given Mach numbers are derived from stagnation flow relations .Investigation is done with flow Mach number 2 as base case . N2 is injected at sonic conditions throughout the investigations with corresponding static temperature of 250k.The injection total pressure to free stream pressure ratio is defined as pressure ratio$(P')$and is taken as 10 in base case .Two cases are investigated, one by changing the pressure ratio while keeping the other parameters same as base case second by changing the free stream Mach number. The geometry is chosen same as that of experimental but with the reduced reference length of 100mm.

Figure 3.3 shows the compression of pressure contour ,Mach contour and wall pressure for jet and supersonic cross flow interaction. As the fuel jet interacts with the supersonic cross flow, a bow shock is produced. As a result, the upstream wall boundary layer separates, providing a region where the boundary layer and jet fluids mix sub sonically. This regions are important in transverse injection flow fields because of its flame-holding capability in combusting situations.[67, 68].Figure 3.3 shows the formation of recirculation zones due to boundary layer separation. The jet upstream recirculation has its importance in promoting auto ignition.

Figure 3.3 a gives the comparison of the pressure contour, Mach contour with an xy plot of wall pressure. The injected gas acts as an obstruction to the primary flow and, as such, produces a shock wave in the primary flow, see Figure 3.3 . A large wake with a low-pressure region forms aft of the injector, as described by Spaid et al.[69] is observed ,see Figure 3.3 .

3.4   Effect of injecting at different angles

In this section effect of injecting fuel at different angles is studied. The inflow conditions and injection parameters are chosen similar to the base case as described in above section. For the given inflow and injection conditions analysis is done for different injection angles ranging from 30 deg to 150deg. Injecting at angle below 90 degrees indicates that fuel is injected into downstream and injecting above 90degrees indicates that fuel is injected against
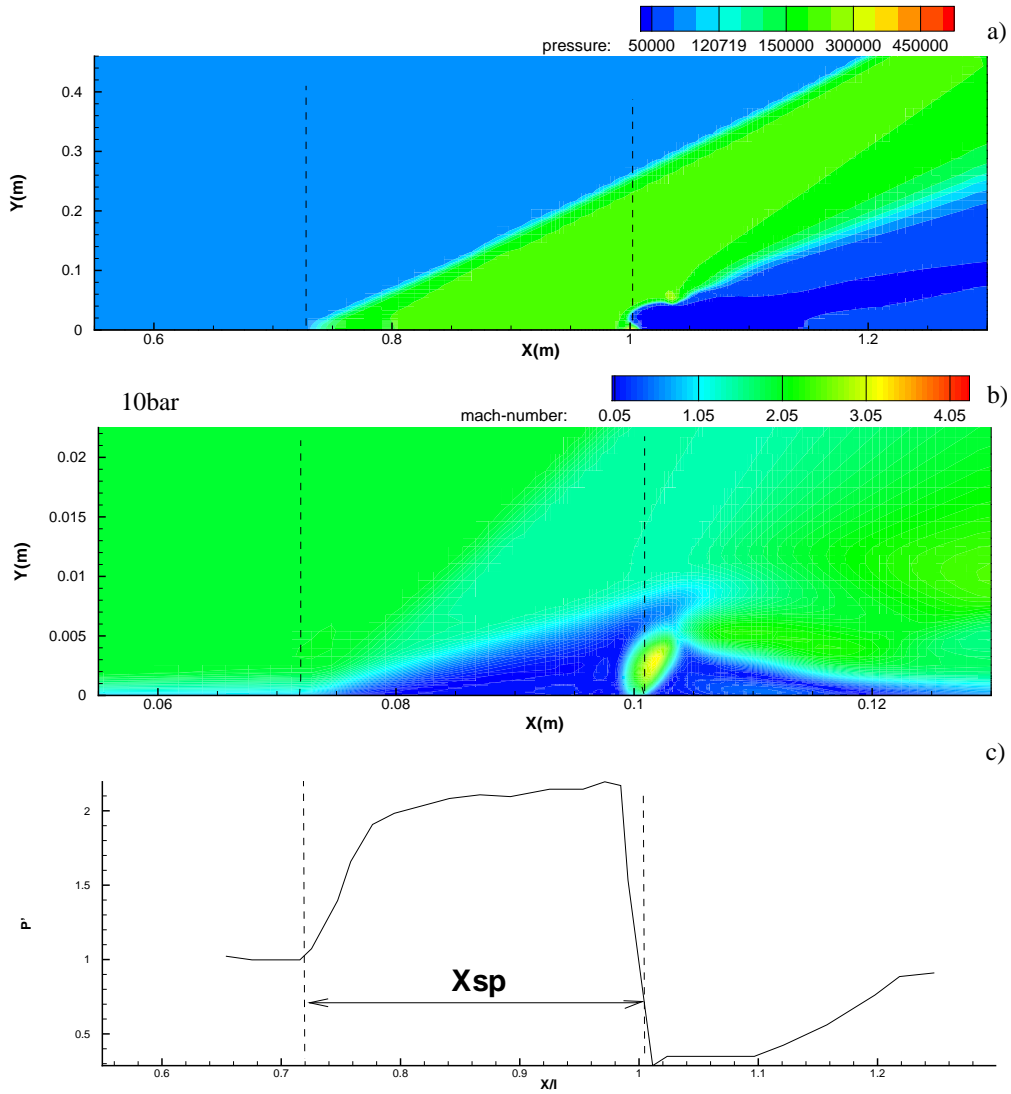
Figure 3.3: Numerical results showing a) Pressure contour b) Mach contour c) Pressure plot

upstream. Upstream separation length and peak pressure is found more in case of normal injection than with inclined injection.

Figure 3.4 shows the predicted Mach contour with fuel injection into downstream. From the Mach contours it is clearly observe that the both upstream and downstream recirculation region are larger for 90 degree injection angle and it got reduces as we decrease the injection angle from 90 to 30 degrees. Inclined injection is likely to reduce or eliminate auto ignition and stabilization because of absence of recirculation regions especially at flight speeds lower than Mach 10.[70]

Also from Figure it can also be observed that as the angle of injection is reduced from 90 to 60 degrees Mach disc partially deformed and inclined towards downstream and when injected at 30 deg with horizontal plate in downstream no Mach disc is observed. The degree
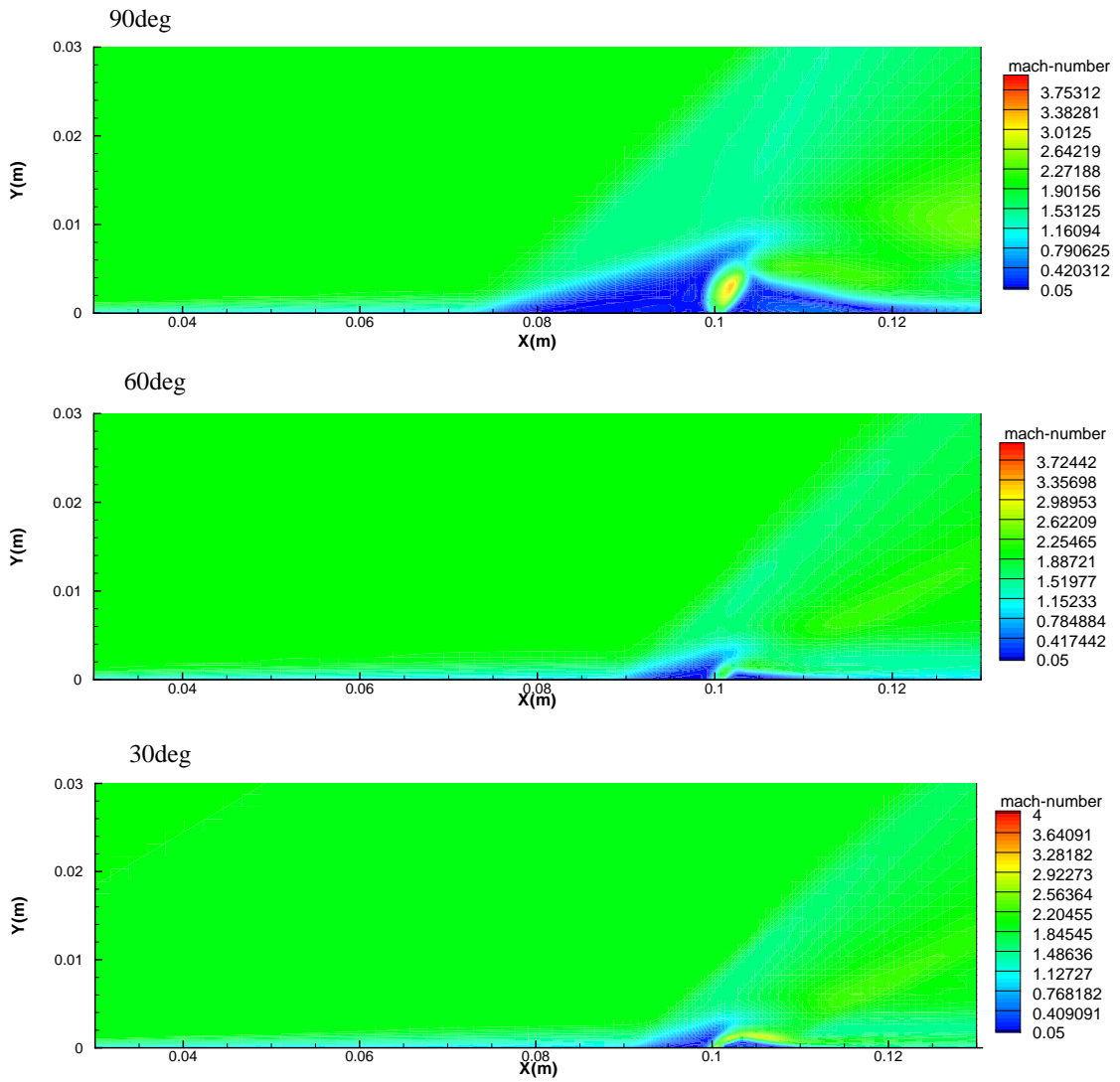
Figure 3.4: Comparison of Mach contours at different injection angles downstream

of separation of boundary layer is less as the fuel is injected at lower angle; this indicates that the shock strength has also reduced.

Figure 3.5 shows the predicted Mach contour with fuel injection against upstream. By injecting the fuel at an angle against the free stream in all the cases there is formation of recirculation region both upstream and downstream of the jet with varying sizes.
With increase in angle of injection from 90 to 120 degrees the upstream recirculation region is minimized, see Figure 3.5. Upstream recirculation region is found slightly larger with 150 deg injection case than with 120deg. Width of the Mach disc has reduced with injection against upstream.
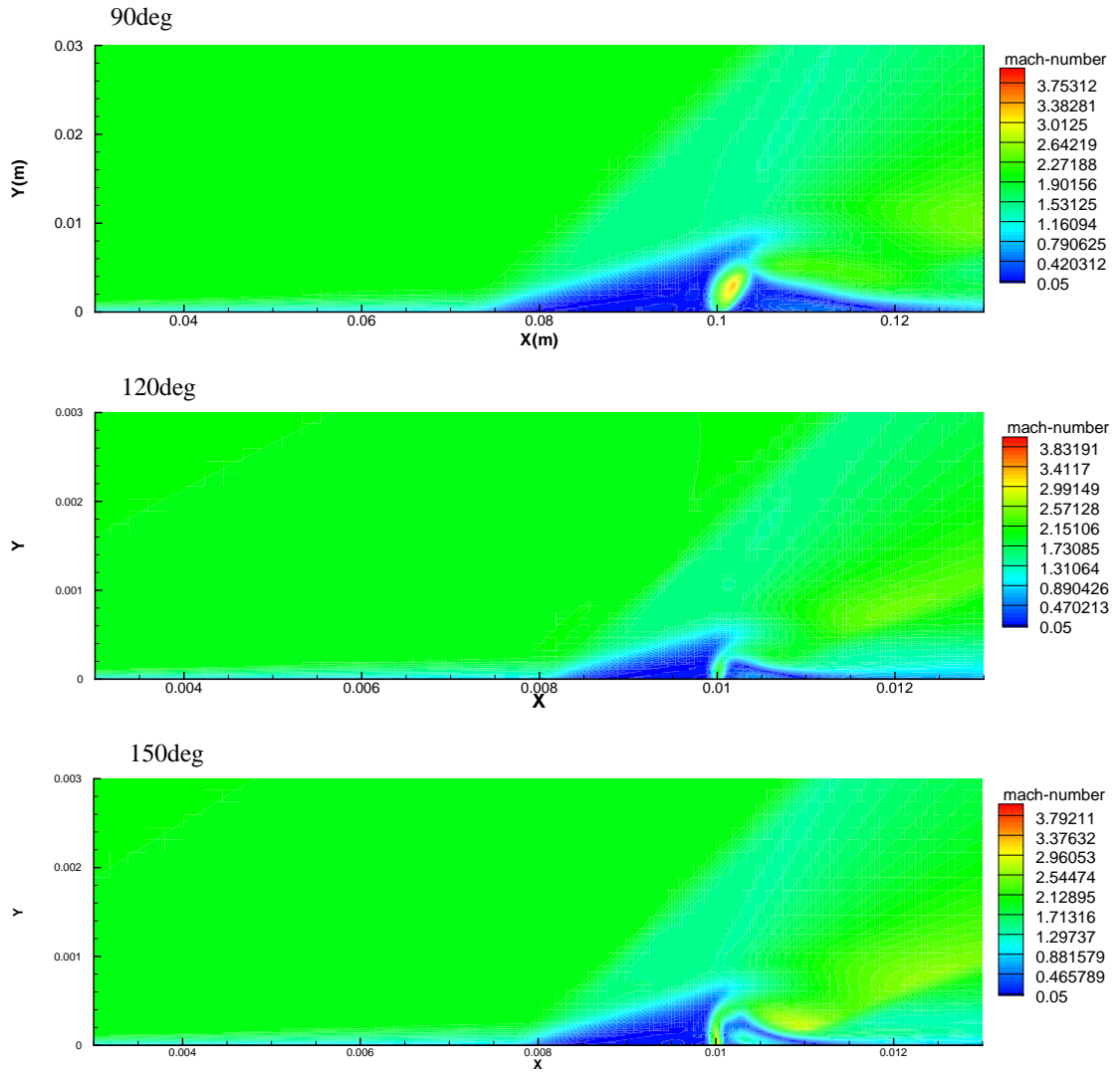
Figure 3.5: Comparison of Mach contours at different injection angles downstream

Figure 3.6 gives the quantitative comparison of wall pressure for all different injection angles ranging from 30 to 150 deg. From Figure it is clearly observed that as the injection angle is decreased from 90 to 30 degrees the peak pressure as reduced. Secondly the length of the upstream separation region as also decreased with increased jet inclination toward downstream. The upstream separation is found more in case fuel injection against upstream than with injections toward downstream. Upstream separation and peak pressure is found more with injection angle of 150 deg than with 120 deg.

The intensity of pressure disturbances upstream of the injection has reduced when the angle of injection is reduced from 90 to 30 degrees. At high flight Mach number the pressure losses due to normal injection will be very high .So it is recommended to use angle injection for flight Mach number greater than 12 [71].

Figure 3.6: Comparison of wall pressure at different injection angles

3.5 Effect of free stream conditions

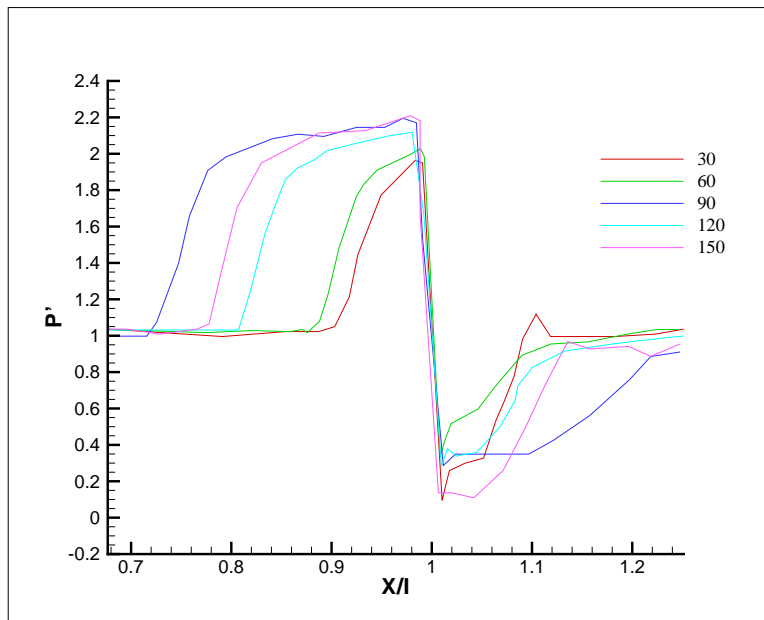Figure 3.7 shows the predicted Mach contour at different inflow free stream Mach number. At higher inflow conditions the jet penetration is found less. From the Figure 3.7 it is observed that the height of the Mach disc got reduced with increase in free stream flow speed .The size of both upstream and downstream separation regions reduced with injection into the high speed flow.

Figure 3.8 shows the corresponding pressure plots for different inflow conditions. From the plot one can notice that, width of the pressure rise upstream of the injector is more at Mach 2 inflow conditions while the concentrated pressure rise is observed with Mach 5 inflow conditions. In all the cases expansion is followed by pressure raise and this expansion is found quick at Mach 5 and is slow at Mach 2.

Figure 3.9 gives the quantitative comparison of wall pressure .Form plot it is observed that the peak pressure is found to be 4bar in case of Mach 5 inflow conditions and the peak pressure is found lower with Mach 2 inflow conditions. The width of the pressure disturbance is found more at lower free stream flow. Pressure downstream of the injector is observed low for the Mach2 inflow condition. Reduction in separation length with simple wall injection system suggests the need of creating additional local recirculation zones especially in higher Mach number flows.
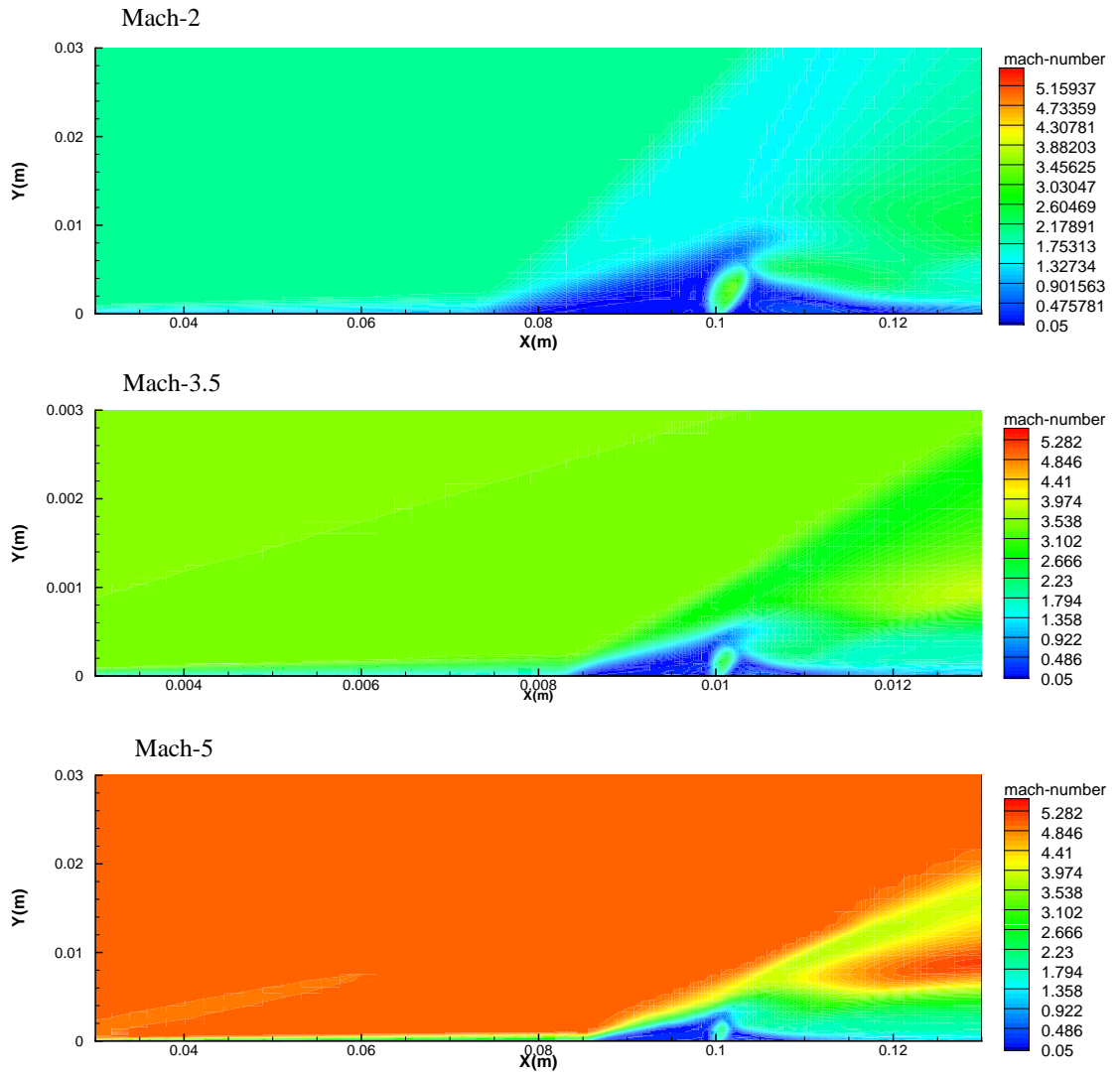
Figure 3.7: Comparison of Mach contours at different inflow conditions

3.6 Effect of injection pressure ratio

In this section effect of the jet pressure ratio is presented. Figure 3.10 shows the predicted Mach contour at different injection pressure ratios. From contour one can notice that with increase in pressure ratio the size of the Mach disc as increased, both the width and height of the Mach disc is found more at higher pressure ratio(Figure 3.10).

Figure 3.11 gives the comparison of pressure contours for different pressure ratios. Both the upstream and downstream injection separation regions are found larger at high pressure ratios. With increase in pressure ratio width of the pressure disturbance upstream has increased. Expansion fans are observed downstream of the injector.

Figure 3.12 gives the quantitative comparison of the wall pressures for different pressure
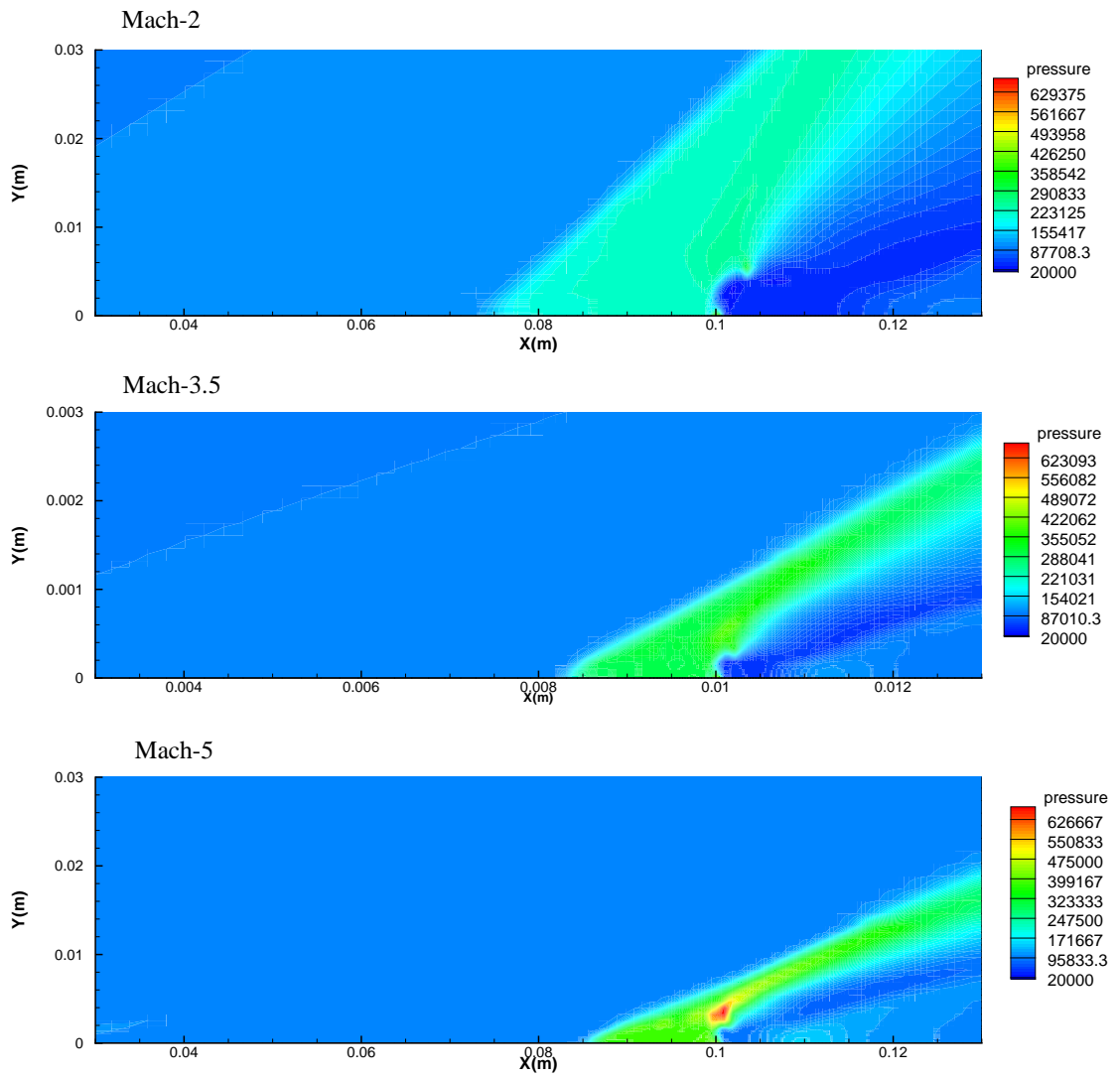
Figure 3.8: Comparison of pressure contours at different inflow conditions

ratios. Both the width of the pressure disturbance upstream and the peak pressure is
observed more in case of higher pressure ratios.
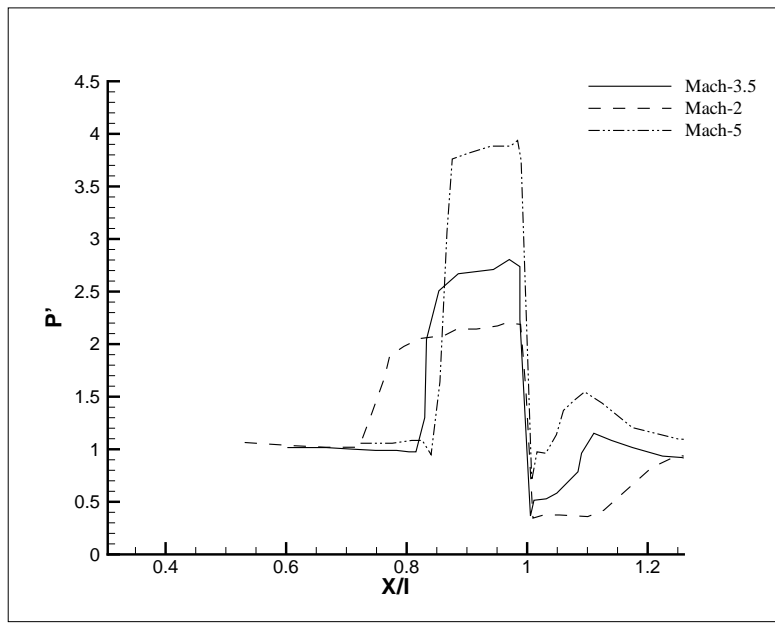
Figure 3.9: Comparison of wall pressure at different inflow conditions
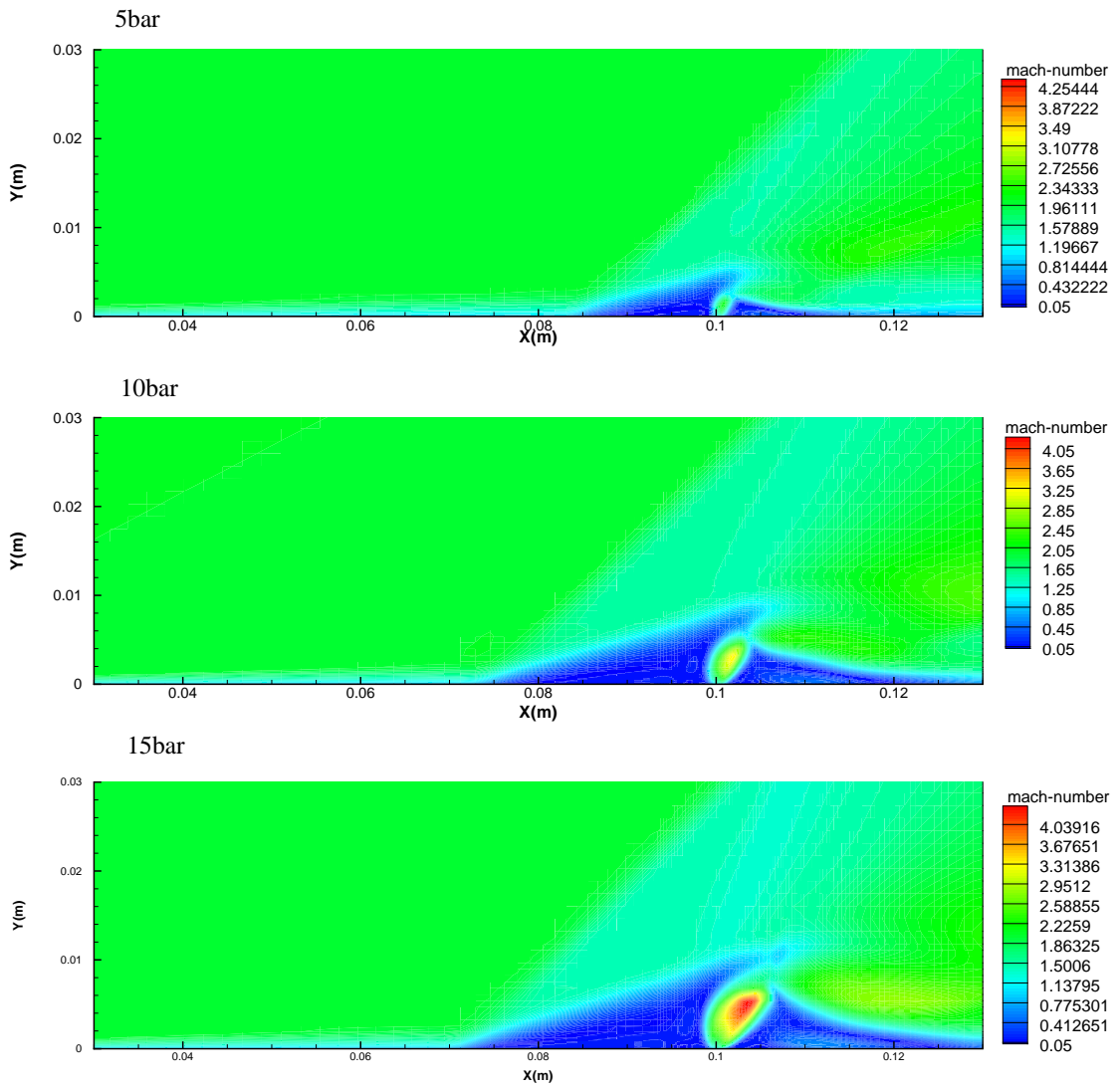
Figure 3.10: Comparison of Mach contours at different injection pressure ratios
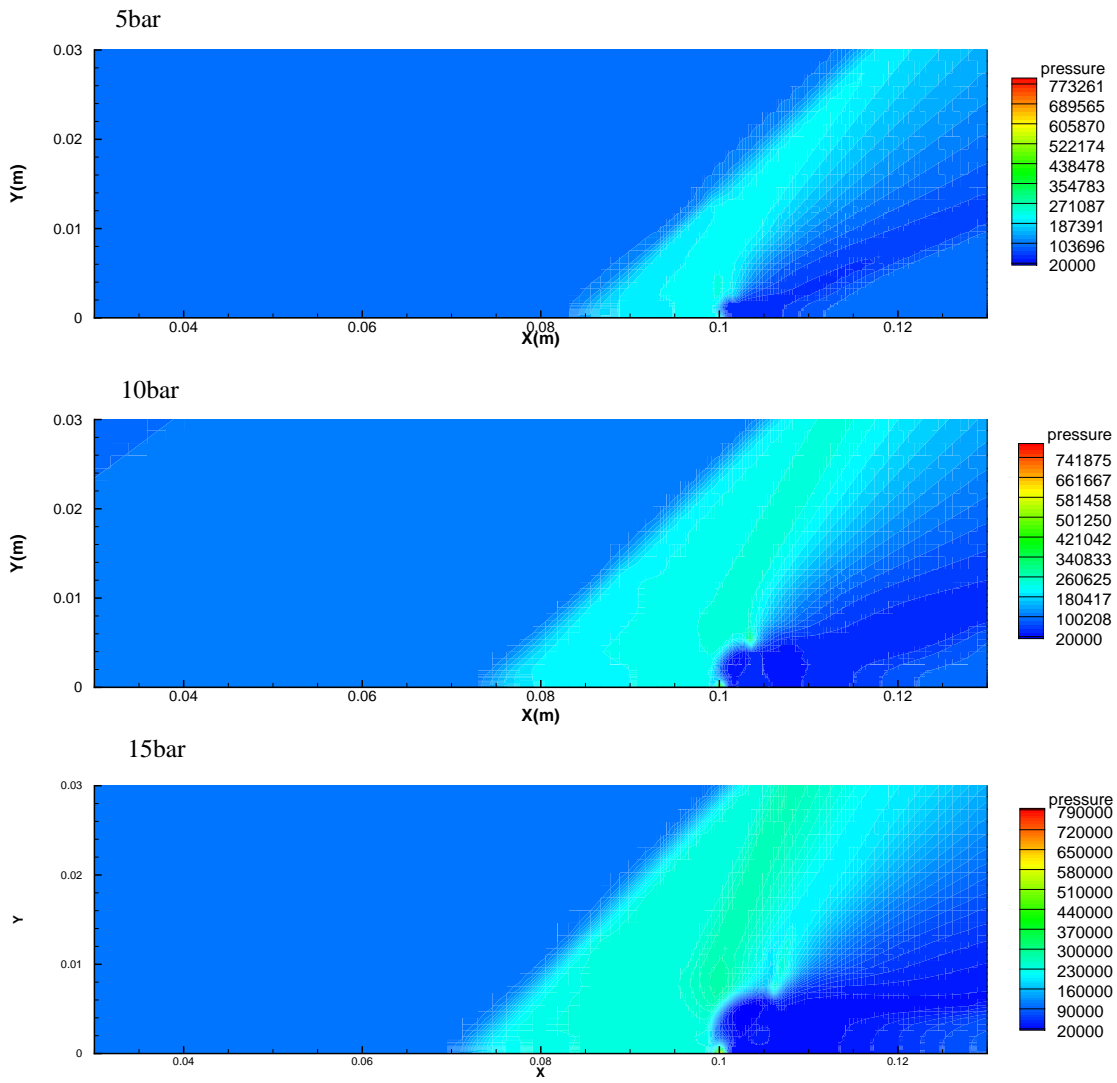
Figure 3.11: Comparison of pressure contours at different injection pressure ratios

37
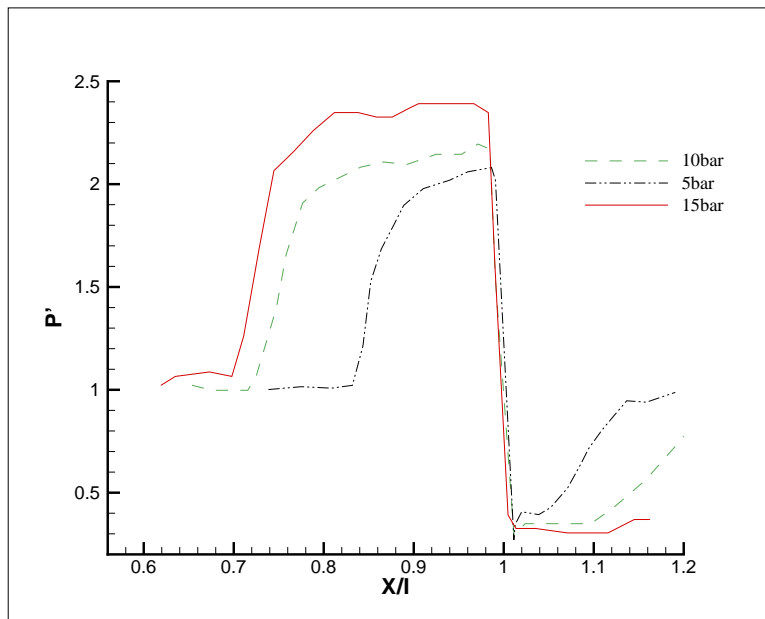
Figure 3.12: Comparison of wall pressure at different injection pressure ratios

Chapter 4

Results and discussion on combustor

4.1 Grid independence study

Computational grid used for the present investigation is shown in Figure 4.1.Numerical simulations are obtained with three different grid sizes: coarse mesh 40000 cells, medium mesh 70000 cells and fine mesh 100000 cells. A fine grid is used near the fuel injector to capture the pressure and temperature gradients due to combustion. Wall Y^+ less than 5 is realized to resolve the gradients near the wall.
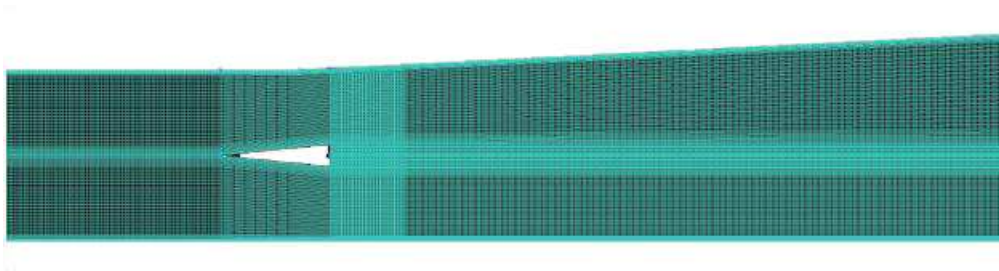
Figure 4.1: Computational grid.

Figure 4.2 shows the variation of hydrogen mass fraction along the center line plotted for different computation grids. From Figure one can notice that the some variation in results is found between coarse and medium mesh but results shown grid independency after 70000 cells and hence all simulations reported herein with medium mesh. Present results are validated with DLR experimental results.
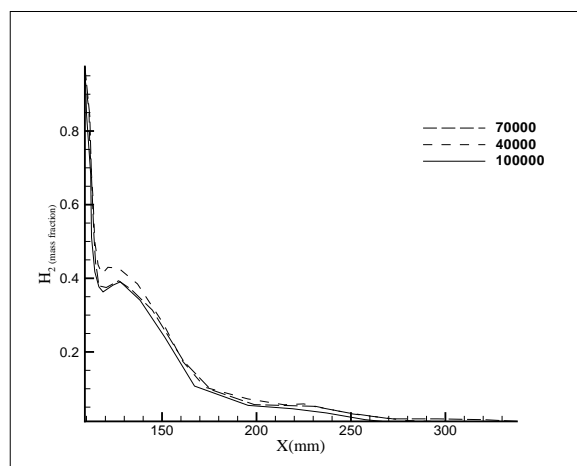
Figure 4.2: H_2 mass fraction along the center line for different grids

4.2 Validation

Accuracy of present numerical model is tested by validating the DLR experimental results available in the literature[33, 34, 35]. Details of DLR scramjet combustor operating conditions are shown in Table 4.2.
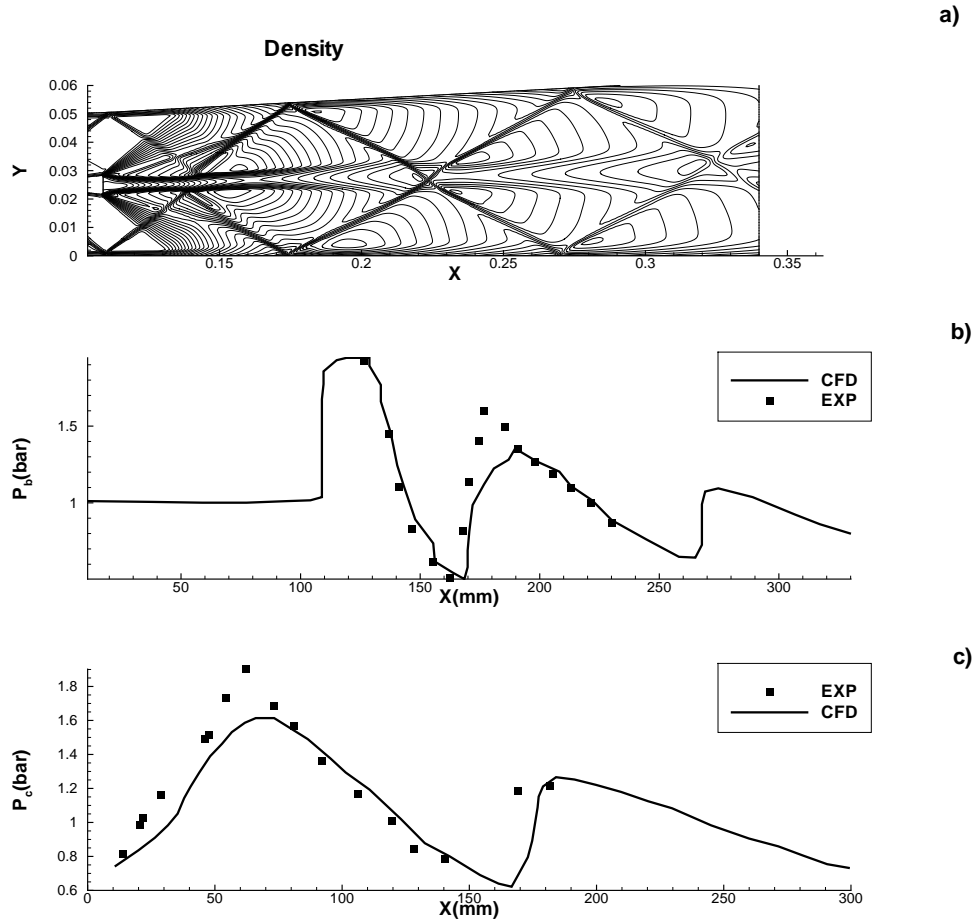
Figure 4.3: Non-reacting flow: (a) Density contours, (b) Bottom wall pressure and (c) Center line pressure.

Figure 4.3(a) show the density contours for non-reacting flow case. Hydrogen fuel is injected parallel to air at sonic velocity ($M = 1$) and considered as inert gas without any combustion. The oblique shocks generated from the leading edge of strut, expansion waves from the base of strut and their reflections from the walls are captured accurately and shown in 4.3. Present results are matching very well with schlieren shadowgraph reported in[36].Figure 4.3(b)and(c), give quantitative comparison between present results and DLR experimental results. Surface static pressure distribution along the bottom wall (Pb) and center pressure (Pc) variation along the combustor are plotted in Figure 4.3(b)and (c) .

Parameters	Air	Hydrogen
Mach number	2.0	1.0
Axial Velocity(m/s)	730	1200
Static Temperature(k)	340	250
Static Pressure(bar)	1	1
density(kg/m3)	1.002	0.097
O_2 mass fraction	0.232	0
$H_2 0$ mass fraction	0.032	0
N_2 mass fraction	0.736	0
H_2 mass fraction	0.0	1
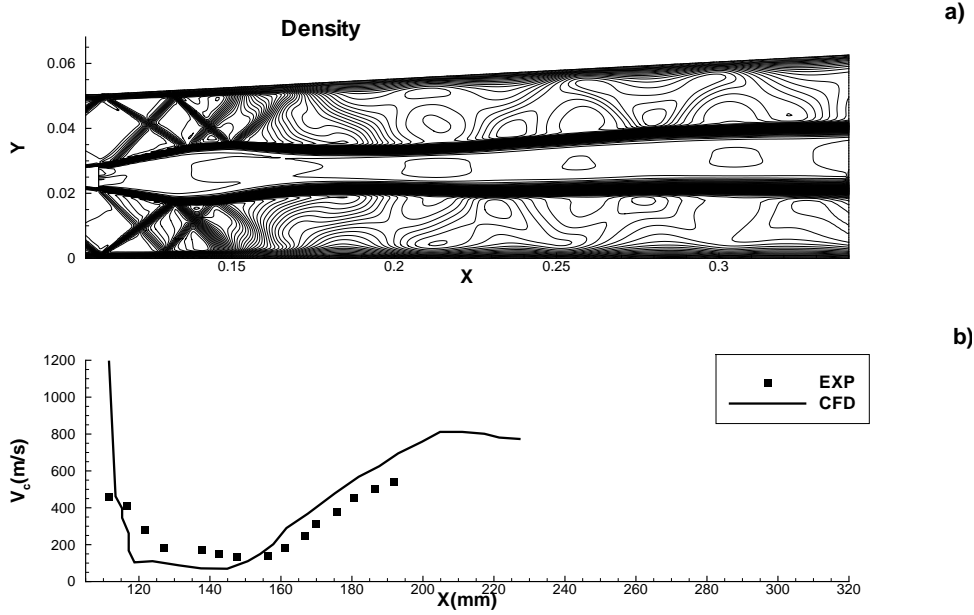
Figure 4.4: Reacting flow: (a) Density contours and (b) Center line velocity.

In Figure 4.3, one can notice sudden raise of pressure due to shock impingement on the wall. The slight deviation between present results and experimental results are observed since walls are treated as smooth surfaces. Also in supersonic experiments probes are placed at a distance to avoid disturbances and shock formation from such measuring devices. The center pressure variation along the combustor has agreed well with the experimental results and slightly underestimated in the strut wake region. Density contours are shown in Figure 4.4(a) for the case of chemically reacting flow. The density has decreased in the reacting flow case compared to non-reacting flow. The shock patterns are weakened significantly in the downstream of combustor due to combustion.

The density pattern in the combustor has agreed well with the DLR experimental re-

sults reported in[36]. The comparison of center velocity with experiment for reacting flow is shown in Figure 4.4(b). The high speed hydrogen fuel sharply decelerated from 1200 m/s (injection velocity of hydrogen) to about 100 m/s within short distance. The axial velocity remains almost constant in the intensive zone of reaction and then gradually increased downstream of the combustor. Present results agreed well with experimental results and slight deviations near the fuel injection due to the approximation of combustion with single step reaction. Also maximum temperature recorded due to combustion is found less than adiabatic flame temperature.

4.3   Significance of divergence angle

Flow field phenomena in scramjet combustor are studied numerically and reported for different design and operating conditions. Hydrogen fuel is injected parallel to air and simulations are performed for chemically reacting flow. The effect of divergence angle and scaling of DLR combustor on performance are reported here. The effect of shocks created by strut and different operating conditions on combustion efficiency are reported.

To know the effect of divergence angle on the top wall of combustor, results are shown in Figure 4.5 for different divergence angles. The operating and geometrical parameters are same as DLR experimental conditions except the divergence angle on the top wall. The Mach contours in the combustor without divergence angle on the top wall are shown in Figure 4.5. From this Figure, one can notice separation bubble formation and sudden fall in Mach number. The strength of the separation region decreased with an increase of divergence angle from 0 to 1.5 degree. No separation region is observed with an increase of divergence angle from 1.5 to 3.0 degree and also smooth shock reflections are observed. From Figure 4.5, one can notice that shock- boundary layer interactions leads to a separation region. Divergence angle provides an increasing cross sectional area along the downstream. This stabilizes the disturbances caused by sudden expansion of flow due to combustion and avoids normal shock formation. Thus diverging area facilitates the free flow of expanding gas without chocking.

Hence sufficient divergence angle has to be provided to avoid sudden drop in Mach number and the boundary layer separation. Diverging area can also be provided by giving divergence angle on both walls. An attempt is made to know the effect of divergence angle of 1.5 degree each on both walls instead of giving 3 degree divergence angle on top wall. The Mach contours in the combustor with a divergence angle of 1.5 degree on top and bottom walls are shown in Figure 4.6. From this Figure, it is noticed that divergence angles accommodates the expanding boundary layer on both walls and flow patterns are symmetric
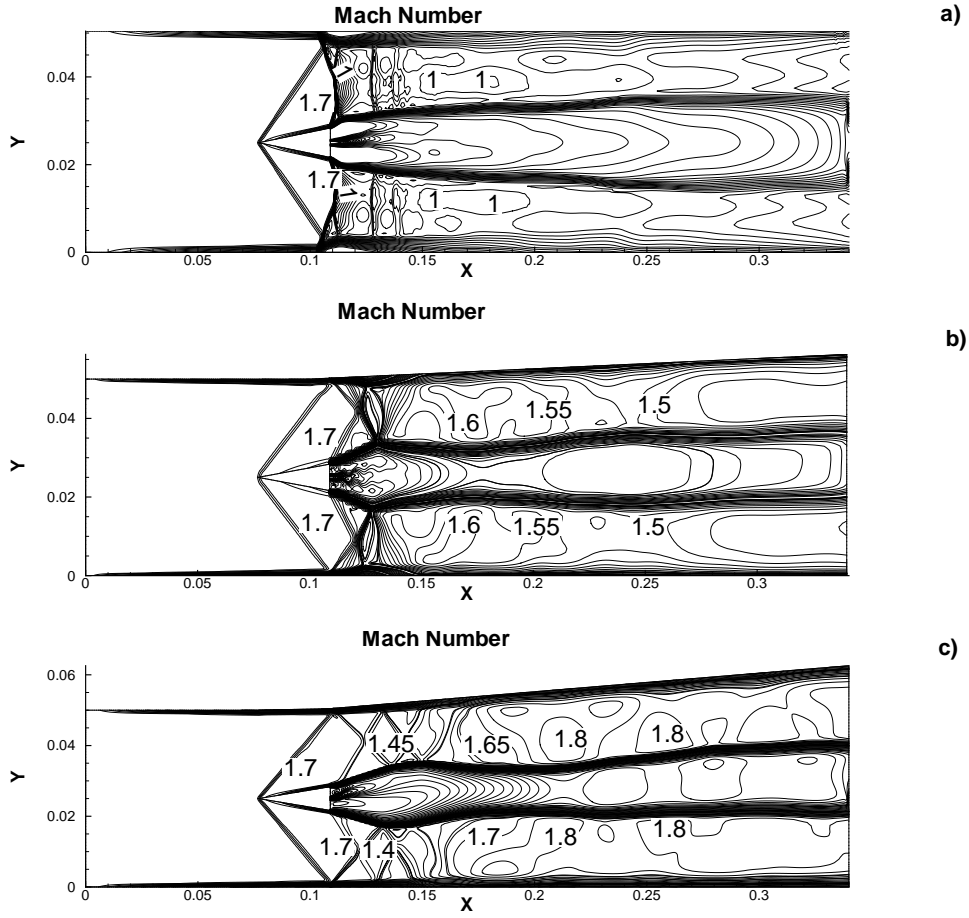
Figure 4.5: Mach number contours for different divergence angles on top wall.

about the center axis of the combustor. The performance of combustor is measured by combustion efficiency (η_c) which is defined as:

$$\eta_c = 1 - \frac{\int_A \rho u Y_{H_2} dA}{\dot{m}_{H_{2_{inj}}}} = 1 - \frac{\dot{m}_{H_2(x)}}{\dot{m}_{H_{2_{inj}}}} \tag{4.1}$$

Where $\dot{m}_{H_2(x)}$ is the mass flux of hydrogen at a given section and $\dot{m}_{H_{2_{inj}}}$ is the mass flux of fuel injected. The combustion efficiency is plotted along the combustor as shown in Figure 4.6 for the cases of 3 degree divergence angle on top wall and 1.5 degree divergence angles on top and bottom walls. From Figure 4.6, the combustion efficiency is higher for the case of divergence angle on top wall compared to divergence angles on both walls because of asymmetric structure provides a better mixing and combustion of fuel. The fuel is burned at a faster rate in case of geometry with 3 degree divergence on top wall than a symmetric combustor i.e with 1.5 degree divergence on both walls. The above analysis shows that the divergence angle on top wall is one of the important parameter have to be considered for

44
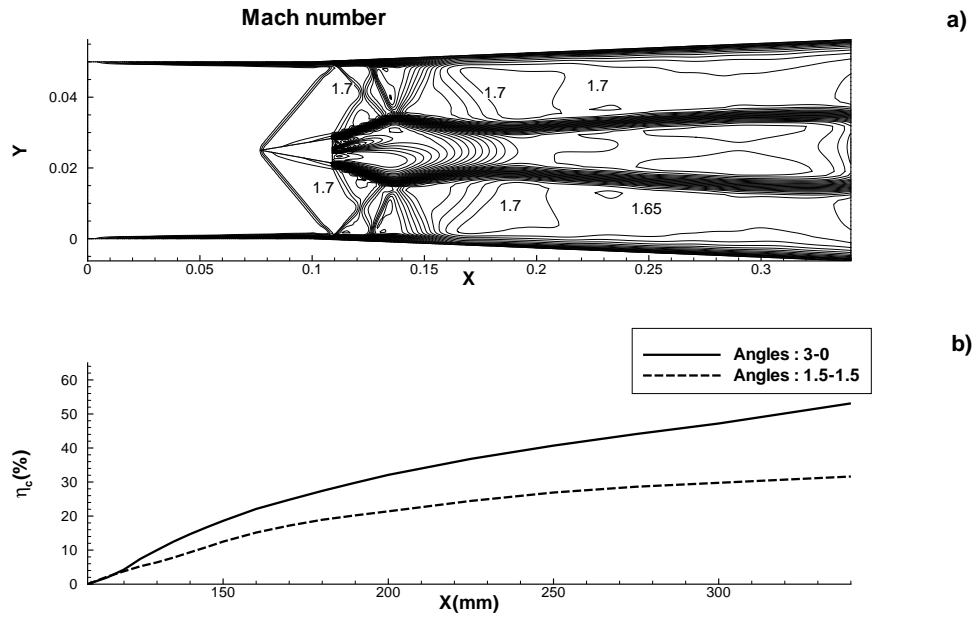
Figure 4.6: (a) Mach number contours with 1.5 divergence angle on both walls. (b) Comparison of combustion efficiency for different divergence angles.

design of scramjet combustor.

4.4 Effect of scaling

To know the effect of scaling height wise on DLR scramjet combustor, corresponding results are shown in Figure 4.7 for different scaling factors. DLR scramjet combustor is chosen as the base model for scaling. The operating conditions are same as DLR experimental conditions. The pressure contours in the combustor are shown in 4.6 for different scaling factors 0.75, 0.6 and 0.5. From this Figure, the flow is steady and smooth shock reflections are observed till 0.6 but the shock interactions become complex with 0.5 scale factor. Sudden fall in Mach number by such interactions is shown in Figure 4.7. Combustion efficiency is plotted along the combustor for different scaling factors as shown in Figure 4.8.

See Figure 4.8, the combustion efficiency of DLR combustor increases with decrease of scaling factor till 0.6. The combustion efficiency of DLR combustor decreased with scaling factor of 0.5 due to insufficient height of the combustor for smooth shock reflections. The above analysis shows that the proper height of the combustor for a given geometry is one of the limiting factors which have to be considered in design of scramjet combustor.

To know the effect of shocks generated from leading edge of strut, combustion efficiency

45
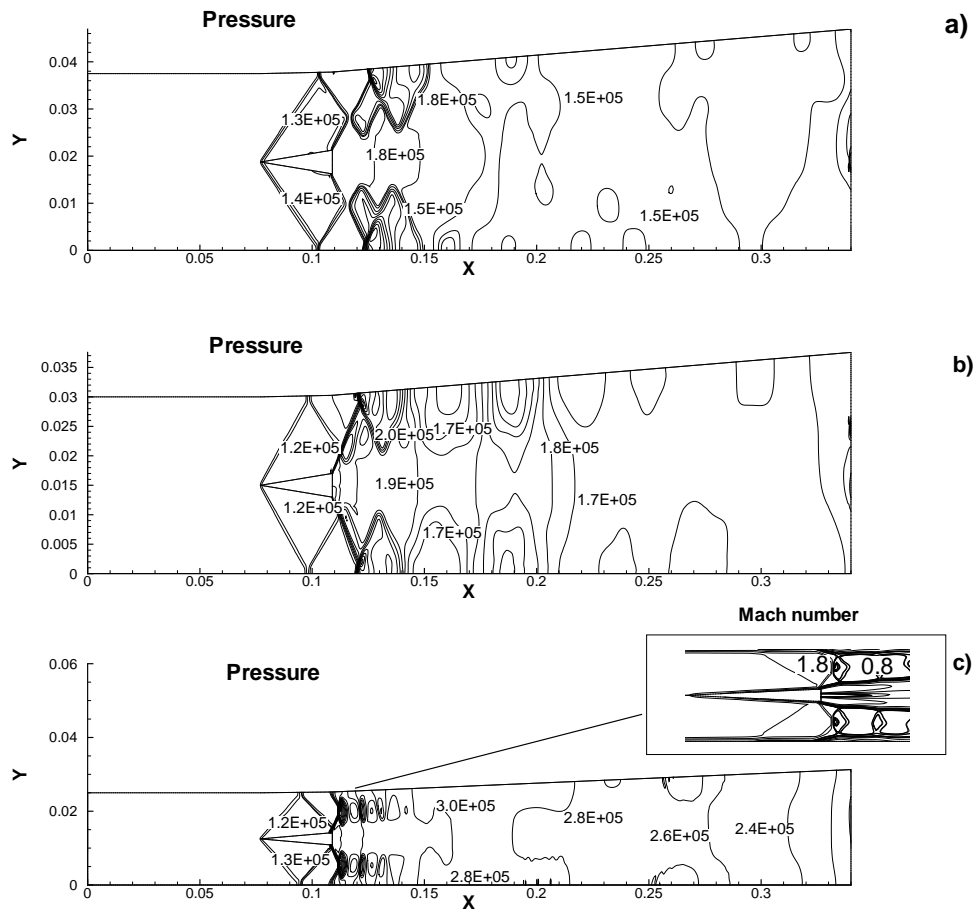
Figure 4.7: Pressure contours for different scaling factors.

is plotted along the combustor as shown in Figure 4.9 for the cases of with and without strut. The operating and geometrical parameters are same as DLR experimental conditions. Hydrogen gas is injected from the strut base. The inlet section of combustor starts from the strut base to avoid the formation of shock generated from the leading edge of strut. From Figure 4.9, combustion efficiency is higher for the case of combustor with strut compared to the case of combustor without strut. The shocks generated from the leading edge of strut enhance mixing and improves the performance of combustor.
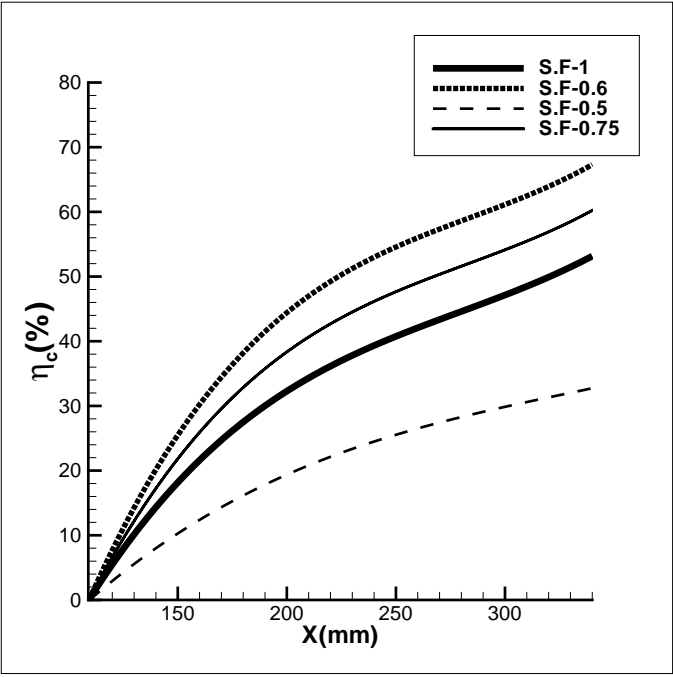
Figure 4.8: Combustion efficiency for different scaling factors.
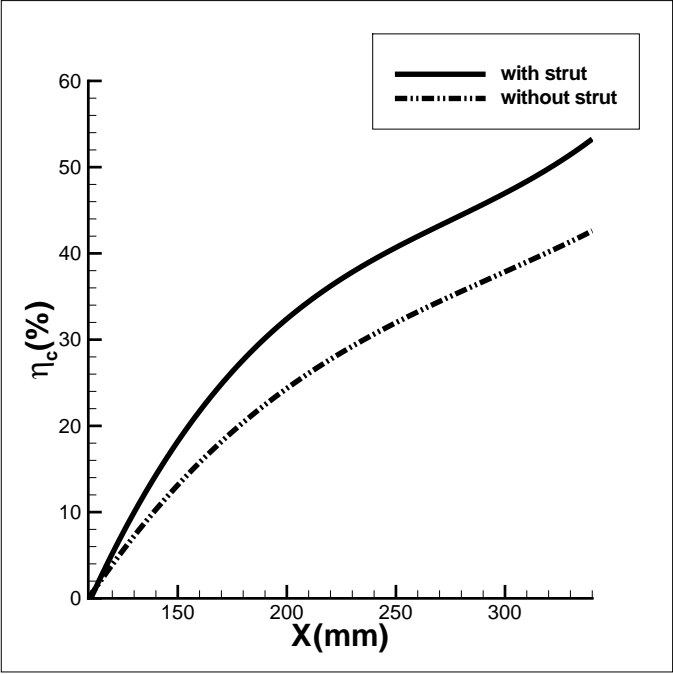
Figure 4.9: Combustion efficiency of combustor with strut and without strut.

47

4.5 Effect of operating conditions
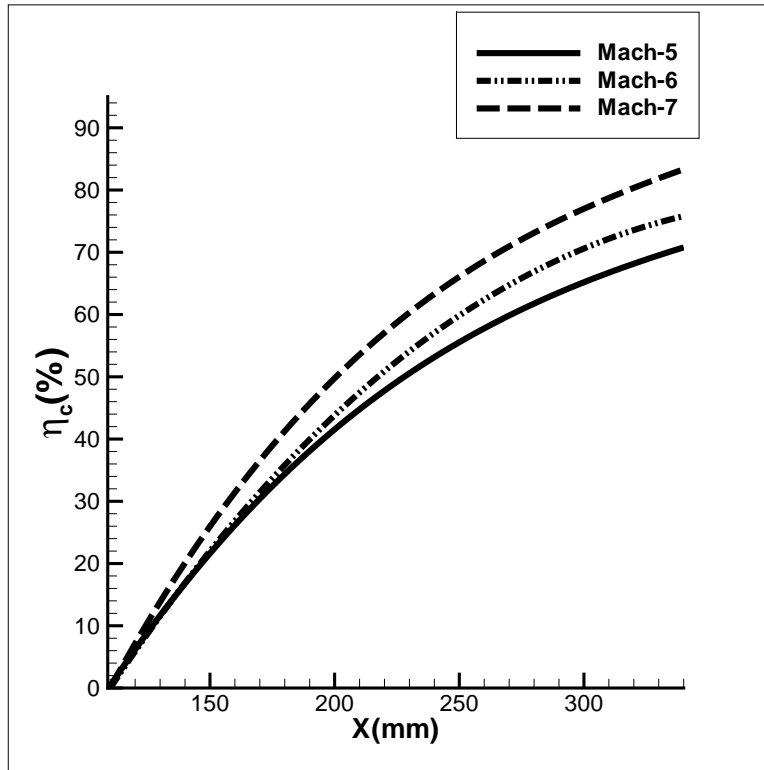
Figure 4.10: Combustion efficiency for different design scramjet inlet Mach numbers.

The inlet conditions of scramjet combustor vary based on the design of scramjet inlet and operating Mach number of the inlet. Recently a new approach was developed by Prakash and Venkatasubbaiah[45] for design of scramjet inlets. Based on this approach the inlet conditions of scramjet combustor are given in Table 5.1 for different design Mach number of scramjet inlet. The combustion efficiency is plotted along the combustor as shown in Figure 4.10 for different inlet conditions as given in Table 5.1. Hydrogen fuel is injected parallel to air at sonic velocity. The combustion efficiency increases with increase of design Mach number of scramjet inlet due to increased pressure and temperature of air at the inlet of combustor. The above analysis shows that pressure and temperature of air at the inlet of combustor are important parameters to be considered for design of scramjet combustor.

Table 4.2: Inlet conditions of scramjet combustor

S.no	Design Mach	Combustor Inlet Mach	Temperature(K)	Pressure(bar)
1.0	5.0	2.16	882	2.595
2.0	6.0	2.45	938	2.935
3.0	7.0	2.78	1104	4.178

4.6 Multiple strut injector
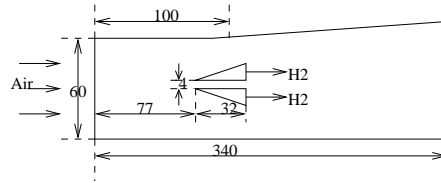
Figure 4.11: Schematic of two strut scramjet combustor.

The geometrical parameters are same as DLR combustor except the strut. The triangular strut has been changed to two right angled struts placed symmetrically about central axis as shown in Figure 4.11. The vertical distance between two struts is 4mm and height of the combustor is 60 mm, strut face is 6mm. In this model air flows between two struts. Density contours of non-reacting flow are shown in Figure 4.12 for single and multiple struts. These results are obtained for design Mach number 5 of scramjet inlet and the corresponding combustor inlet conditions are given in Table 5.1.
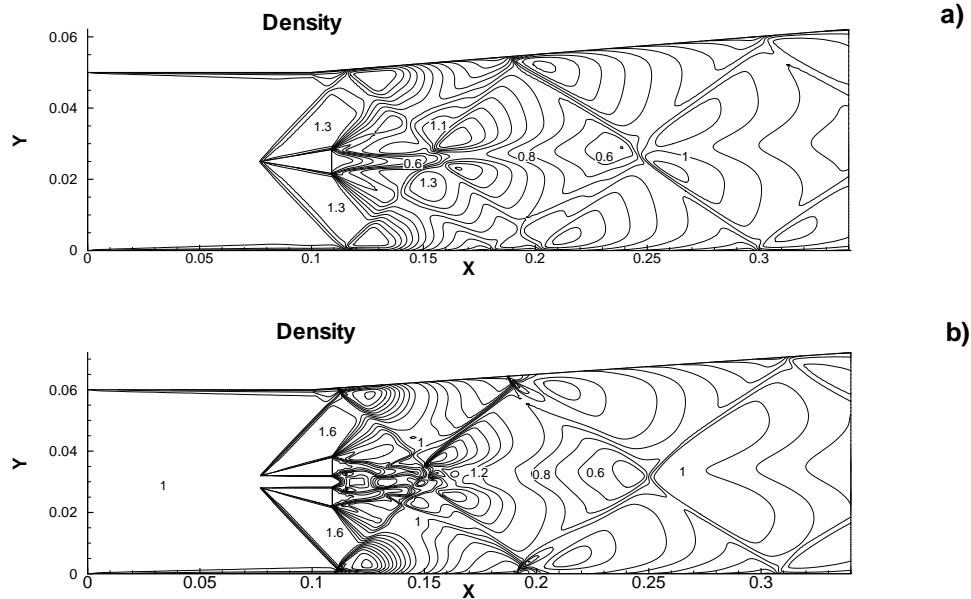
Figure 4.12: Density contours of non-reacting flow: (a) Single strut and (b) Two struts.

From 4.12, low density recirculation region is formed near two struts compared to single strut. As the air exit from the passage between two struts got expanded and created the low density recirculation region between two fuel jets. This helps in initial fuel-air mixing and further mixing is enhanced by shocks in downstream. The combustion efficiency is plotted along the combustor as shown in Figure 4.13 for single and multiple struts. The combustion

efficiency is higher for multiple struts compared to single strut due to better mixing of fuel and air.
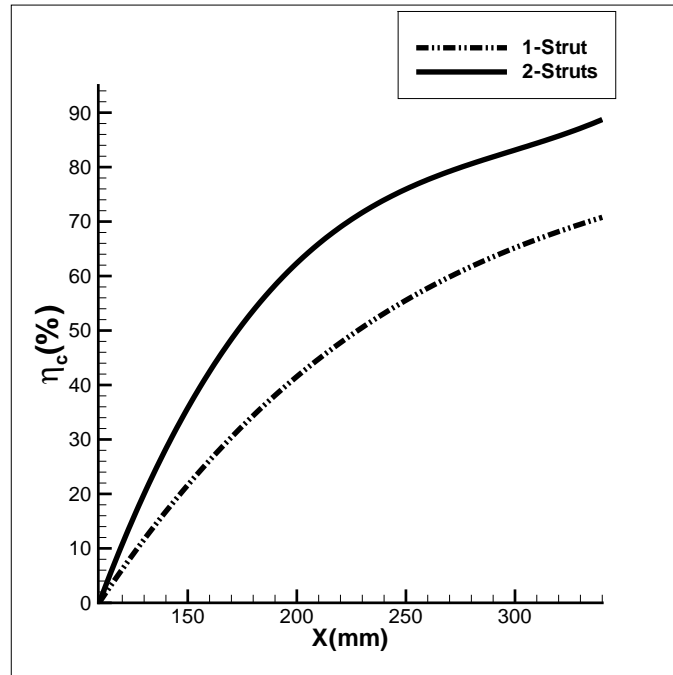
Figure 4.13: Comparison of combustion efficiency with single strut and two struts.

Chapter 5

Results and discussion on Nozzle

5.1   Grid independence study

Computational grid for the present investigation is generated using ICEM CFD. At wall grid is densely clustered and interior cells are made relatively courser by giving the suitable node pattern. Closest node to the wall is set at height of 0.01mm [47].Three grids of different levels of density with total cell count of 38000, 110000, and 200000 are generated to ensure the grid independence. Figure 5.1 shows the pressure on ramp surface plotted for these three grids.
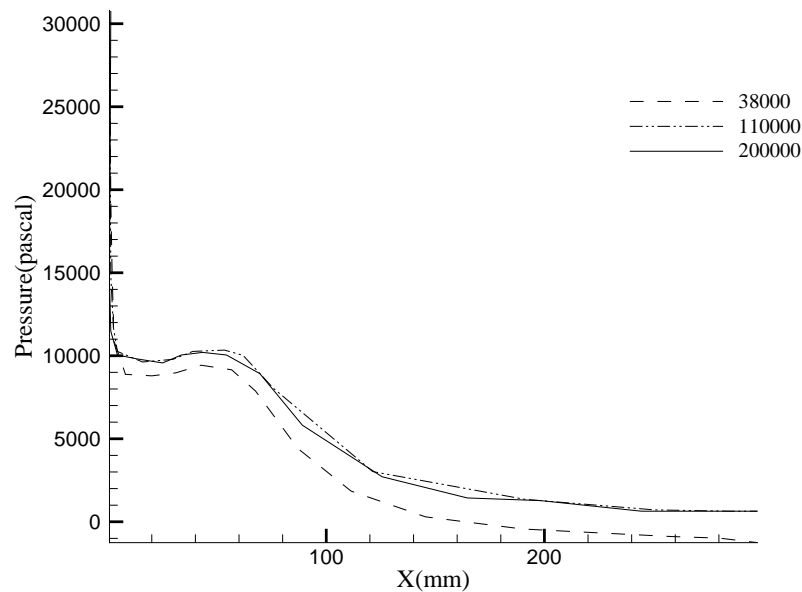
Figure 5.1: Plot showing ramp surface pressure comparison for different grids.

It is found that there is variation is pressure between coarser and medium grids and Pressure profile is almost coinciding between 110000 and 200000 grids. For the analysis in the present work 110000 grid is used.

5.2   Validation

Inflow conditions are taken as declared in experiment for validation study. Experimental nozzle inflow Mach number 1.78 with total temperature of 475K and total Pressure of 172K Pascal are employed at inlet. The free stream conditions taken from wind tunnel flow measurement are as follows, static temperature 58K, the static pressure1596.07 Pa, with Mach number 6. Flow variables at outflow are extrapolated from the interior. Walls are treated as adiabatic and no slip condition is imposed on nozzle surface.

Figure 5.2 gives the quantitative comparison of computation and experimental results at horizontal distance x =3.567h, 5.833h, 10.833h. The pressures are normalized by a reference pressure of 6895Pa, and the vertical distances are normalized by a reference length of 5.08 mm as reported by [64]. The results obtained from are matching very well with the experimental results. The code is able to capture the flow physics as well shown in Mach contour (Figure 5.3).

At the region of interaction between free stream and internal flow field shear layers are formed. Figure 5.3 shows the formation of lower and upper shear layers where the nozzle flow is interacting with the external flow. The interaction of the outward turning jet with external flow causes the jet plume external shock wave. One barrel shock is generated from the edge of expansion surface and another from the trailing edge of cowl.

The upper shear layer turned parallel to the lower shear layer from the point of interaction of oblique shock wave. These two shear layers remained parallel after x=0.85m .Thus from the above Mach contour it is seen that the computation domain is sufficiently large to capture completely developed flow field.

The design of the expanding surface or ramp of SERN nozzle plays a key role in the scramjet propulsion system because most of the thrust force generated from this surface. The cowl is positioned with an angle to take the advantage of expanding gas and to produce the thrust out of it. In the process of extracting thrust from this surface there is chance of decrease in overall thrust as the thrust produced from ramp surface may decrease. The cowl with an angle decreases the pressure on the ramp surface. Geometry from nozzle entry to the exit of cowl is called internal nozzle. The length of the internal nozzle is an impor-

tant parameter to extract the thrust from expanding gases. There should be good balance of thrust production from both internal and external nozzle to generate maximum overall thrust and lift force per unit weight of vehicle. Length of the internal nozzle also plays a major role in stability of vehicle from pitching. Using larger cowl may also decrease the lift force even though some thrust force is added. Overall length of nozzle should be chosen such a way that thrust produced for unit weight must be optimized. Careful studies of behavior of thrust and lift profiles under different operating conditions for a given geometric change is also important to study.

Figure 5.4 gives the clarity of lift and thrust forces. From Figure 5.4 it is clear that the x component of the force acting on nozzle surface is what thrust force is and the negative y component is the lift force.

The total force component(F_i) in any direction $'i'$ is the sum of the pressure force and viscous force in that direction.

$F_i = F_p i + F_v i$

Where F_i is the component of force in any direction $'i'$,

Fpi is the component of Pressure force in any direction $'i'$,

Fvi is the component of viscous force in any direction $'i'$,

5.3   Effect of Geometric parameters

5.3.1   Effect of cowl length

Figure 5.5 shows the variation of thrust and lift force with respect to cowl length . In description of physical model one can see that the chosen length of the horizontal cowl wall as 2 times the height(h) of the nozzle inlet. For the present investigation this length is varied from 1h to 3h.From Figure 5.5 one can notice that by increasing the internal nozzle from 1h to 3h length thrust force has increased. Lift force is in decreasing mode and the rate of decrease in lift force increased when the length is increased beyond 2h. The increase in thrust force is because of increase in pressure on ramp surface due to additional cowl length. With increase in length of the cowl the more pressure acts towards the gravity from the cowl inner surface and contributes to negative lift. If the lift gain from ramp surface is not sufficiently high than lift lost from cowl surface overall lift decreases.

Still further increase in nozzle length may contribute more to thrust force but it also increases the weight of vehicle and decrease the lift force, secondly another consideration is use of longer internal nozzle may lead to stability problems since pitching moment gets effected [57].So the length should be designed keeping in consideration the fore body and inlet shape along with thrust and lift consideration.

5.3.2   Effect of cowl angle

Figure 5.6 shows the variation of thrust and lift force with respect to cowl angle. From Figure 5.6 one can notice that by varying the cowl angle there is not much effect on thrust force and Lift force has increased significantly. Even though some amount of thrust force is added from cowl surface but because of divergence angle on cowl pressure of gasses expanding on ramp wall may decreased. Thus by giving the larger cowl angle even though thrust generated from cowl surface increases but the thrust contribution from the ramp surface has reduced thus creating whole effect on overall thrust.

When angle of the cowl increases the negative lift from its surface decreases and positive lift from the ramp surface also reduces. Here in this case loss in positive lift is less than that of negative lift from cowl surface thus overall lift has increased.

5.3.3   Effect of nozzle Length

Figure 5.7 shows the variation of thrust and lift force with respect to nozzle length . From Figure one can notice that with increase in ramp length there is slight increase in thrust and lift forces but it also adds negative effect of increased weight of vehicle. This shows that certain length of nozzle is sufficient for particular case to captivate and take full advantage of high pressure combustion exit gases.

It is seen that there is increase in lift force with increase in ramp length because of extra expanding surface contributing to force against gravity. The length of the ramp should be chosen to obtain maximum thrust per unit weight according to the requirement.

5.3.4   Effect of ramp Angle

Figure 5.8 shows the variation of thrust and lift force with respect to ramp angle.From Figure one can notice that by increase in ramp angle from 15 to 20 deg there is significant increase in thrust force and there is not much variation in thrust force after that .This shows that expanding of gases at certain rate gives better advantage and optimum thrust. Optimum angle depends on the conditions of gases at nozzle entry. The increase in thrust is due to contribution of axial force from the angled cowl surface.

The normal component of force on nozzle surface against gravity is what the lift force is. As the ramp angle is increased x-component of force increases and y-component decreases. Thus lift force is found is decreasing when ramp angle is increased from 12 deg to 22.5 deg . As the ramp angle increases pressure on the ramp wall decreases thus causing the lift to fall down.
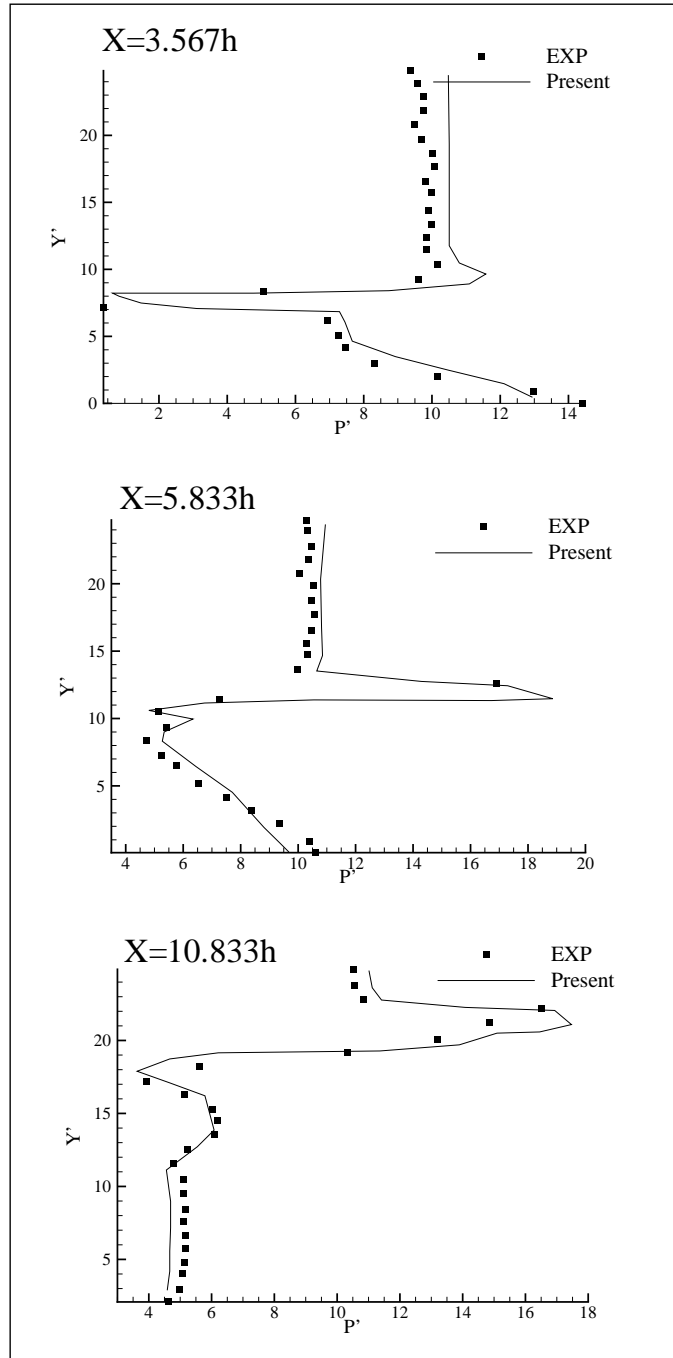
Figure 5.2: Comparison of pressure between experimental and numerical at different X-locations.
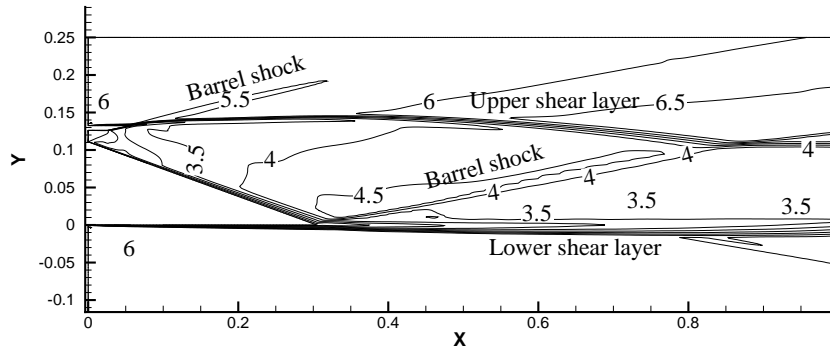
Figure 5.3: Mach number contour showing interaction between internal and external flow field.
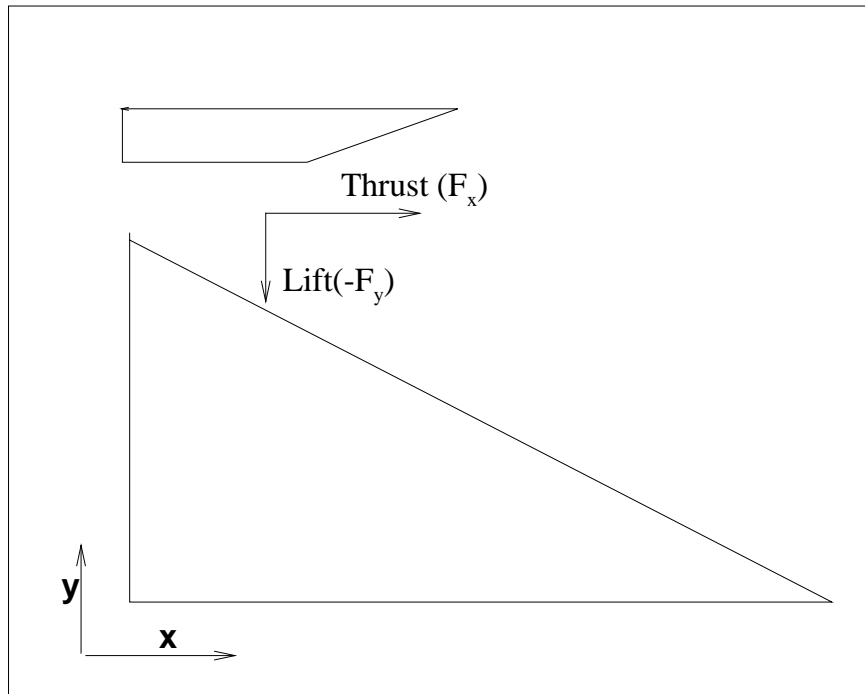
Figure 5.4: Geometry showing force components.

56
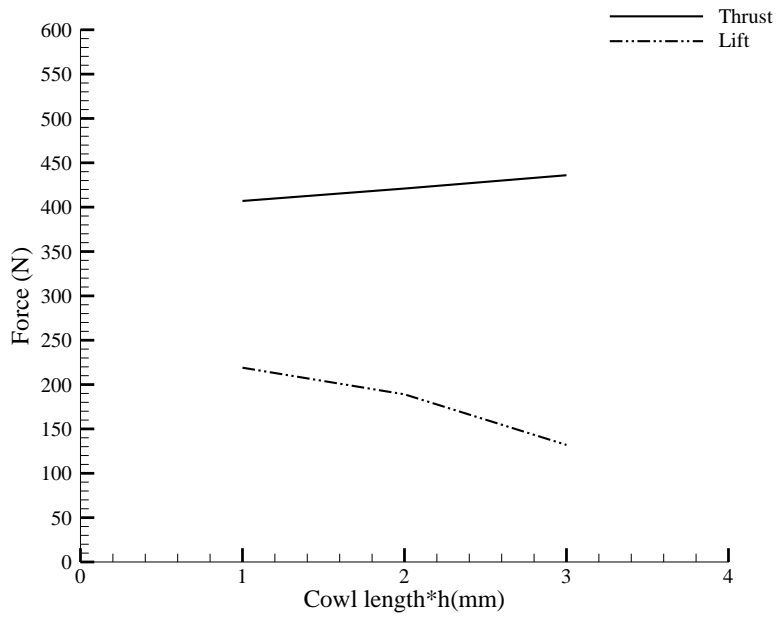
Figure 5.5: Variation of lift and thrust force with respect to length of internal nozzle.
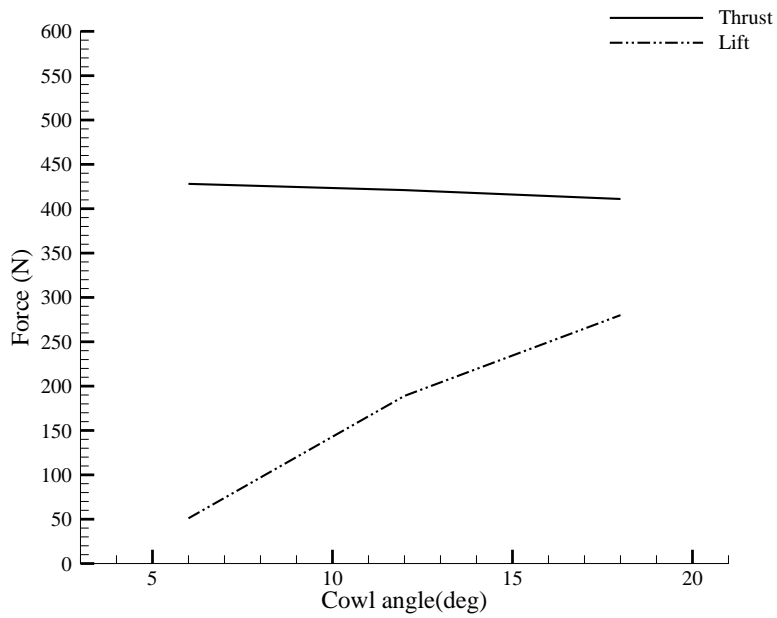
Figure 5.6: Variation of lift and thrust force with respect to cowl angle.
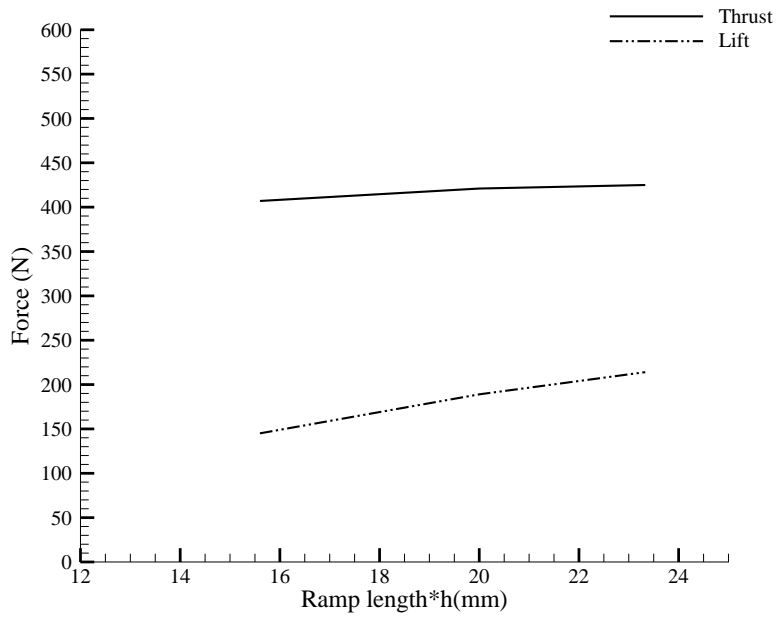
Figure 5.7: Variation of lift and thrust force with respect to Ramp length.

Figure 5.8: Variation of lift and thrust force with respect to Ramp angle

58

5.4 Effect of operating conditons

Table 5.1 gives the information of different operating parameters .The free stream static pressure is taken as 6090 Pascal and the static temperature as 230K .The free stream flight Mach number and the corresponding combustor exit conditions are given in Table 5.1 below.

Table 5.1: nozzle Inflow Conditions

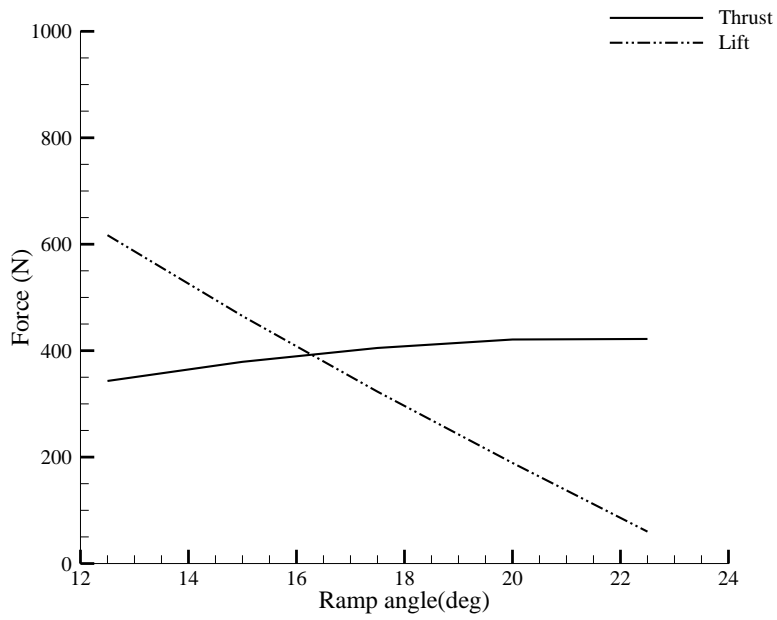| Free stream Mach	Mach	Total Pressure(pascal)	Static pressure(pascal)	Total temperature
5.0	1.76	676645	123887.3	725
6.0	2.13	1343794	128303.2	869
7.0	2.55	3021767	134493.5	1014.3
8.0	3.05	6485027	148175	1183.3

Figure 5.9 shows the mach contours for different operating conditions. Barrel shocks are formed with all the operating conditions .Barrel shocks are formed under all the operating conditions .Flow is completely developed within shorter length in case of lower flight speed. At higher operating conditions barrel shock has moved towards downstream and flow is not fully developed within the chosen domain. The angle at which these shocks formed varied with nozzle inflow conditions. As the inflow mach number of the nozzle is increased, barrel shock is formed at greater angle from ramp surface.

5.4.1 Effect of cowl Length

a)Thrust:

Figure 5.10 shows the variation of thrust force with cowl length under different operating conditions. The rate of increase of thrust is found more at higher operating conditions. Under all operating conditions thrust force is found increasing with increase in cowl length. In case of mach 5 flight mach number as length is increased from 1h to 2h and from 2h to 3h the rate of increase of thrust force is almost same. As the operating mach number is increased some difference in rate of increase in thrust is found .
Under mach 6, 7 and 8 operating conditions rate of increase of thrust is more when length is increased from 1h to 2h than when length is increased from 2h to 3h. Since at inflow higher operating conditions initially a small change increase in cowl length will give more benefit and the advantage of increasing cowl length decreases as it is increased further.

b)Lift:

Figure 5.11 shows the variation of lift force with cowl length under different operating conditions. As the cowl length is increased from 1h to 2h the following changes are ob-

served. Lift force is in decreasing trend under all operating conditions in our investigations and this decreasing rate is more when operated at higher Mach number. When the length is increased beyond 2h the rate of decrease in lift force has changed. This show that increasing the cowl length may increase the pressure on the ramp wall and enhance the thrust but it also shows the negative effect on lift force. The decrease in lift force may be because the negative lift created by cowl inner surface dominating the extra positive lift added by ramp surface.

It is clearly seen that cowl plays a major role in stability of vehicle. The lift force should be kept within the limit according to the fore body and inlet geometry to avoid pitching of the vehicle.

5.4.2   Effect of cowl angle

a)Thrust:

Figure 5.12 shows the variation of thrust force with cowl angle under different operating conditions. From above Figure 5.12 it is found that as the cowl angle is increased thrust force decreased. Thrust force is more when operated at higher Mach number. Under all the flight Mach number thrust force is in similar decreasing trend when cowl angle is increased from 6 to 12 degrees. The rate of decrease of thrust force is found more at higher Mach number when cowl angle is increased beyond 12 deg. This may be because; it is difficult to retain the flow along the cowl surface with higher divergence angle when the flow speed increases.

b)Lift :

Effect of cowl angle on lift force is studied numerically at different operating conditions. Figure 5.13 shows the variation of lift force with cowl angle under different operating conditions. It is found that lift force is more at higher flight Mach number. The slope of the lift vs. cowl angle line between cowl angle 6 and 12 found more in case of Mach number 5 and Mach6.Some change is also observed in rate of decrease in thrust when cowl angle is increased beyond 12 degrees.

It is found; the rate of decrease in lift force is found more initially and decreased with further increase in cowl angle also proves initial small changes will show grater effect. Also flow accelerating at higher speed along the cowl angle shows less negative effect on lift generated from the ramp surface.

5.4.3   Effect of nozzle Length

a)Thrust:

Figure 5.14 shows the variation of thrust force with cowl angle under different operating conditions. As previously discussed as the nozzle length is increased thrust force increases but along with that also weight of vehicle increases. For nozzle operating at Mach5, Mach6 the rate of increase in thrust force is same when ramp length is increased from 15h to 20 h and from 20h to 24h,where h is the height of the nozzle inlet. The rate of increase in thrust force for ramp length between 15h and 20h is found increasing as the Mach number is increased. Since higher operating conditions are able to capitalize the extra nozzle length in more effective in extracting thrust .For Mach 7 and Mach 8 conditions there is slight fall in rate of increase in lift force when the ramp length is increased beyond 20h shows that by increasing the nozzle length further leads to drop in generation of thrust per unit additional weight. So length of nozzle should be limited considering thrust per unit weight.

b) Lift force:

Figure 5.15 shows the variation of lift force with ramp length under different operating conditions.From figure one can notice that with the increase in length of the ramp is increased from 14h to 23.33h lift force increased .At any particular ramp length lift force found more at higher operating conditions. The increase in lift is because of the contribution of added extra surface.

5.4.4   Effect of ramp angle

a)Thrust:

Figure 5.16 shows the variation of thrust force with ramp angle under different operating conditions. From the 5.16 one can notice that thrust force increasing with increase in ramp angle up to certain limit and then it starts decreasing. Since expanding the gases further and further by increasing the ramp angle does not contribute much to the thrust force as pressure exerted on the ramp wall decreases. Gases should be accelerated with proper ramp angle to get maximum benefit.
The trend in 5.16 shows, maximum thrust may obtain at lower ramp angle as the operating Mach number increases. For Mach 5 and Mach6 operating conditions thrust force is in increasing trend as the ramp angle is increased up to 22.5deg. For Mach 7 and Mach8 operating conditions thrust force is in increasing trend up to ramp angle equals 19.5 deg and 16 deg respectively.

b) Lift:

Figure 5.17 shows the variation of lift force with ramp angle under different operating conditions.From the Figure 5.16 one can notice that as the ramp angle is increased between 12 to 20 deg the lift force found decreasing at greater rate than when operated above 20deg.It is also found that the rate of decrease in lift force is more at higher operating conditions. As the ramp angle is increased lift force decreases because the pressure on the ramp wall decreases due to over expansion of gases.
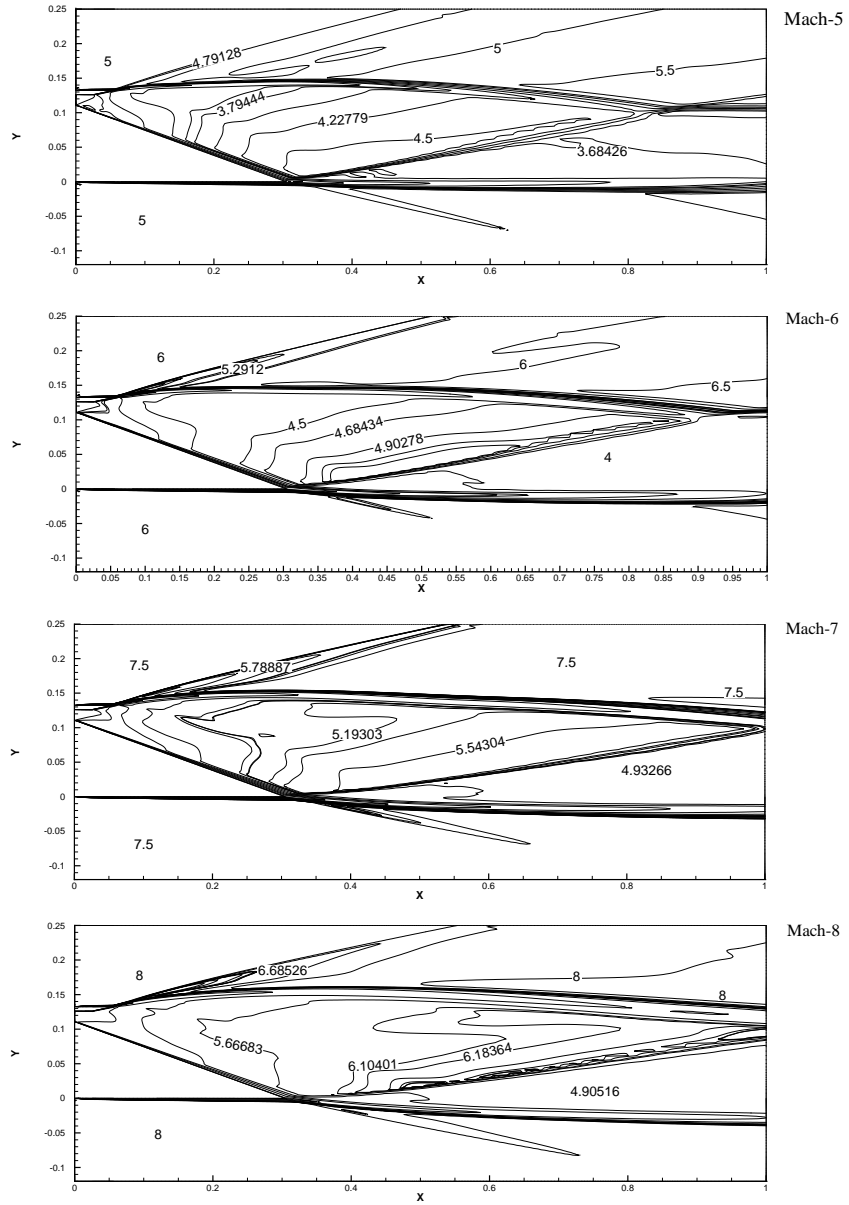
Figure 5.9: Mach contours at different operating conditions.

63

Figure 5.10: Variation of thrust force with respect to cowl length under different operating conditions.

Figure 5.11: Variation of lift with respect to cowl length under different operating conditions.

64

Figure 5.12: Variation of thrust force with respect to cowl angle under different operating conditions.

Figure 5.13: Variation of lift force with respect to cowl angle under different operating conditions

65

Figure 5.14: Variation of Thrust force with respect to ramp length under different operating conditions.

Figure 5.15: Variation of Thrust force with respect to ramp length under different operating conditions.
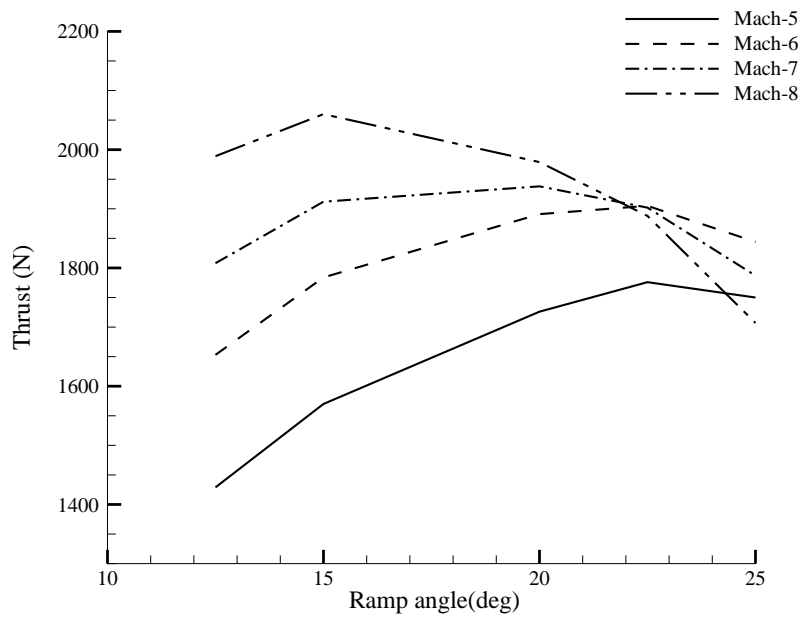
Figure 5.16: Variation of Thrust force with respect to Ramp angle under different operating conditions.
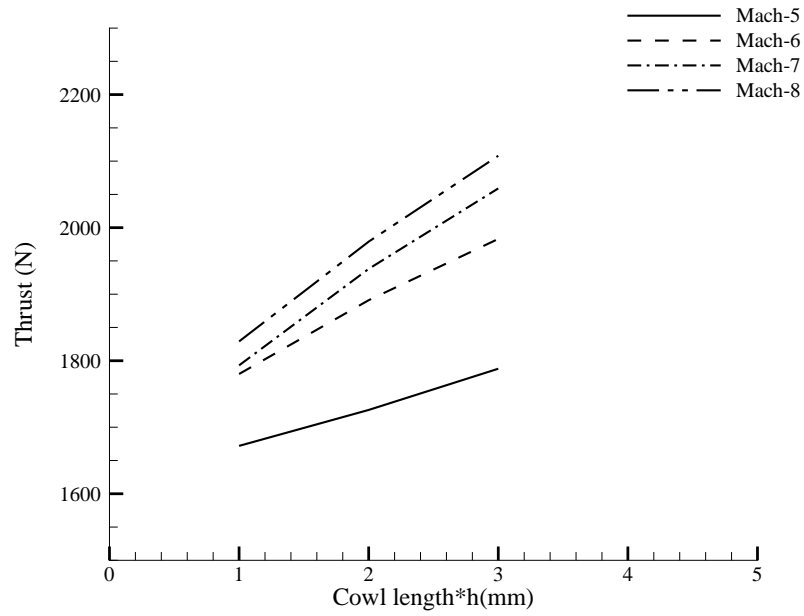

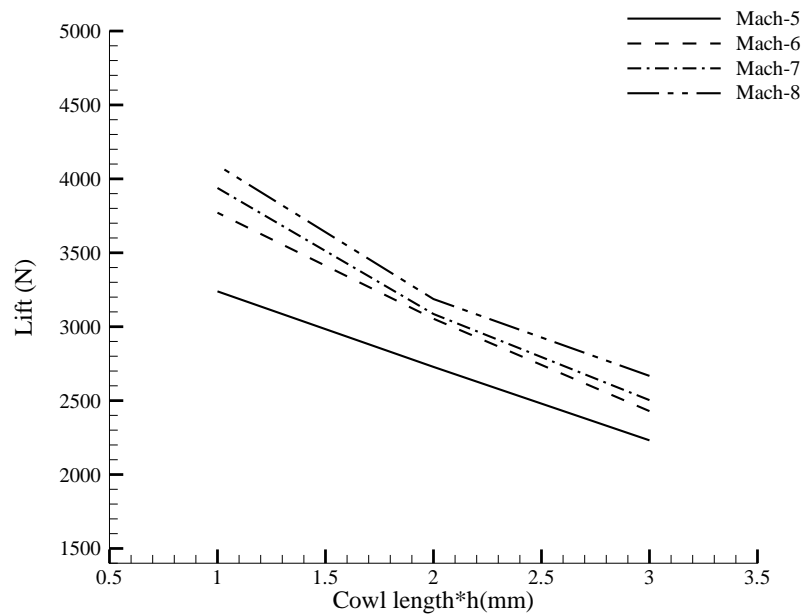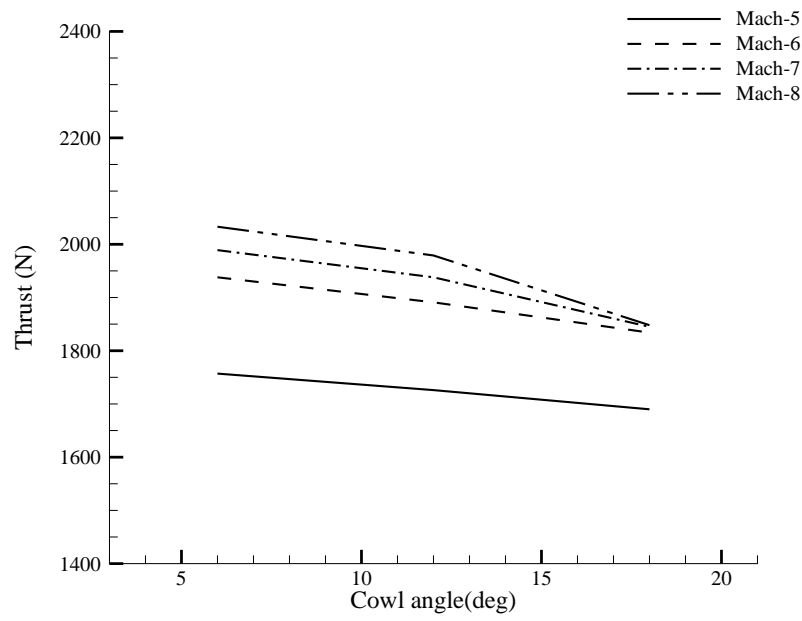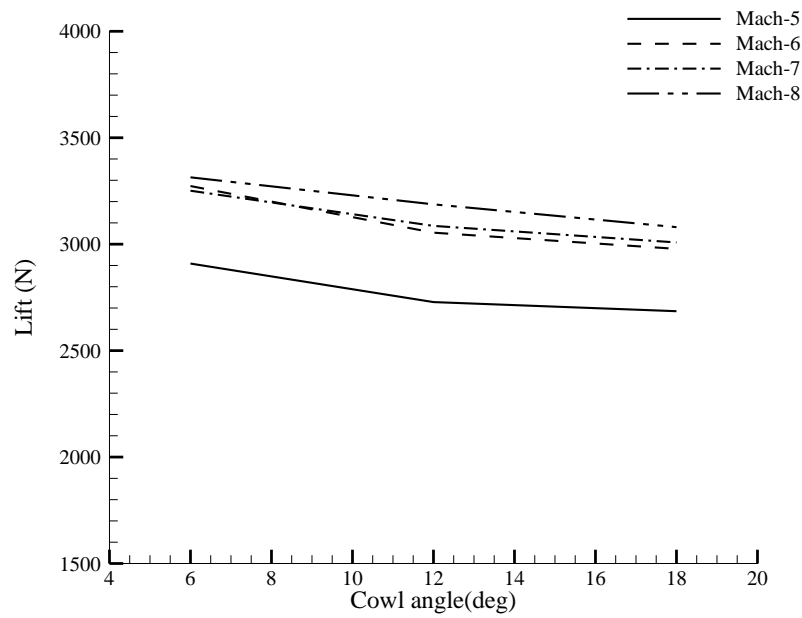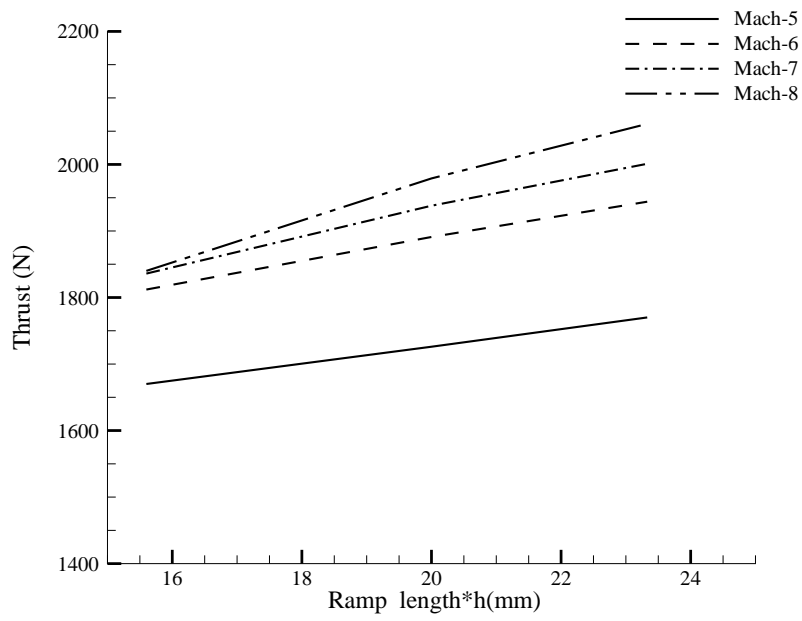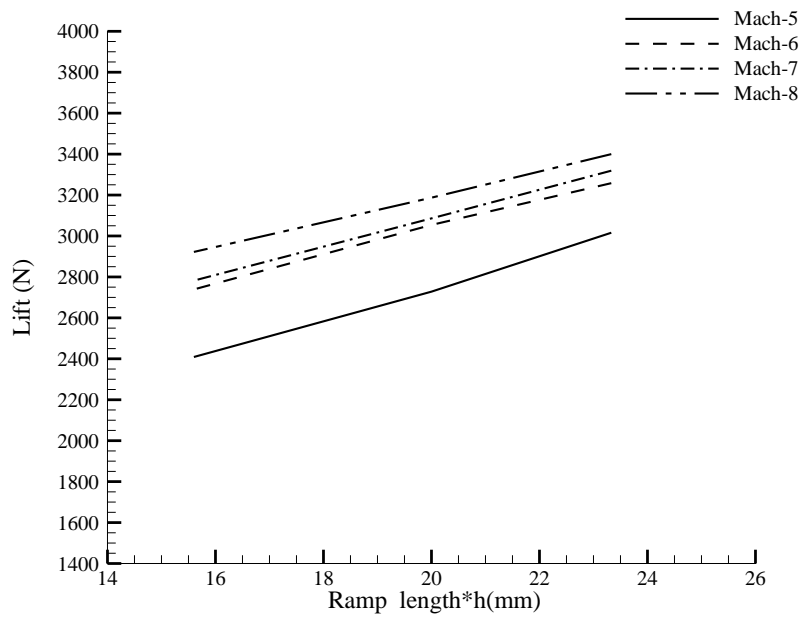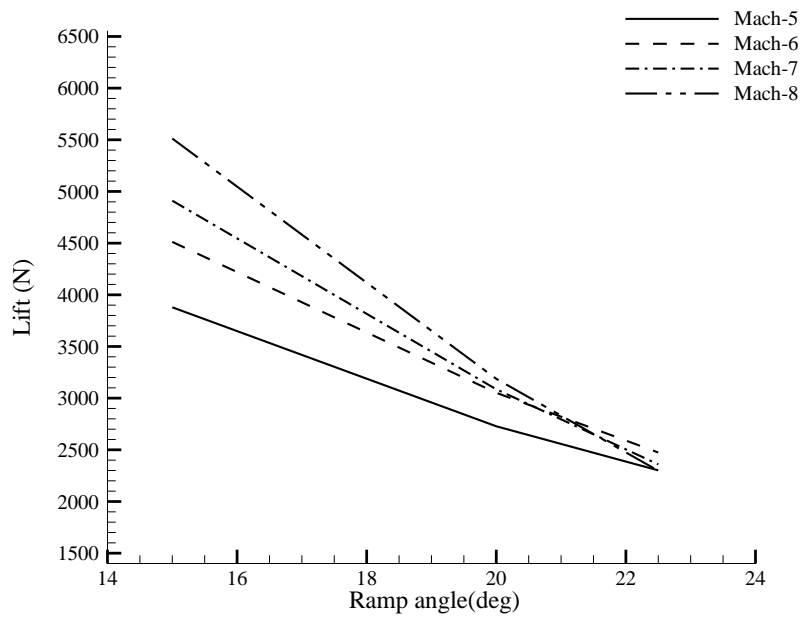Figure 5.17: Variation of Thrust force with respect to Ramp angle under different operating conditions.

67

Chapter 6

Conclusions

Numerical study has been carried out in three phases. In first phase investigations are done on transverse fuel injection system, in second phase investigations are done on scramjet combustor, in final phase numerical investigation are carried out on expansion system. Following conclusions are derived from the present investigation:

i)Fuel injection:

- With increase in the free stream Mach number the separation length has reduced and the wall peak pressure has increased.

- With increase in pressure ratio both the separation length and the wall peak pressure has increased. Also the height of the Mach disc has increased.

- By injecting fuel at an angle into downstream resulted in decrease in separation length and wall peak pressure. The more the jet inclined toward the wall in downstream reported lower peak pressure and separation region.

- By injecting fuel at an angle against upstream resulted in deformation of Mach disc and also the separation length. More the jet injected against the upstream resulted in high peak pressure. But the larger separation length is reported with normal injection.

ii)Combustor:

- The divergence angle on the top wall avoids the sudden fall in Mach number and accommodates the expanding boundary layer.

- Scaling the DLR combustor height wise improved the performance till 0.6 scale factor and any further reduction in dimensions resulted in normal shock formation.

- Present results shown mixing and combustion are enhanced by shocks generated from the leading edge of strut.

- Combustor shown better performance with increase in pressure and temp of vitiated air.

- A modified combustor with two struts fuel injection system shown better performance compared to single strut combustor.

iii) Nozzle :

- With increase in cowl length thrust force increased and major change in lift force is also observed. The rate of increase in thrust force is more with initial increment in cowl length from 1h to 2h and the rate has decreased with further increment in length. Also at higher operating conditions rate of change in performance for any change in cowl length is more than operated at lower Mach number.

- As the cowl angle is increased slight decrease in thrust force is felt in present range of investigation. At higher flight Mach number increase in cowl angle beyond 12 degrees shown increased rated of fall down in lift.

- Thrust force increased with increase in ramp length. The rate of increase is found decreasing as the length of nozzle increases.

- With increase in ramp angle thrust force increase up certain angle and this angle is less high when operating conditions are high.

Present simulations are able to capture the flow field characteristics such as shock/boundary layer interactions, shock reflections and combustion phenomena. Interaction between internal and external flow field are also captured well and are in good agreement with experimental. The present analysis gives inputs for design and development of scramjet propulsion system.

Chapter 7

Future work

Three dimensional modeling gives the scope of designing various strut shapes which enhances the Flame holding and mixing features. Availability of high performance computers gives the scope of integrating the full flow path and refine the existing design. Since turbulence is three dimensional in nature, three dimensional simulations gives more realistic results. Modeling detailed reaction mechanisms gives closer prediction of experimental results.

References

[1] Phillip T. Harsha, Lowell C. Keel, Dr. Anthony Castrogiovanni, Robert T. , "X-43A Vehicle Design and Manufacture", block AIAA 2005-3334.

[2] Jacobsen, L Gallimore, S Schetz, J OBrien, "Integration of an aeroramp injector/plasma igniter for hydrocarbon scramjets", block Journal of Propulsion and Power, 19(12),(2003)170-172.

[3] Huber, P. W., Schexnayder, C. J., and McClinton, C. R, "Criteria for Self-Ignition of SupersonicHydrogen-AirMixtures " *NASA* TP 1457,(1979).

[4] Ben-Yakar et.al. Numerical study on supersonic combustion with cavity-based fuel injection , Proceedings of the Twenty-Seventh International Symposium on Combustion, Combustion Inst.,Pittsburgh, 21732180(1998).

[5] Chung-Jen Tam I, Robert A. Baurle, Numerical Study of Jet Injection into a Supersonic Crossflow, AIAA Paper (1999)99-225.

[6] Fric, T. F., A. Roshko , Vortical structure in the wake of a transverse jet, Journal of Fluid Meachanics ,pp. 1-47, (1994) 0022-1120.

[7] Billig, F. S., Research on supersonic combustion, Journal of Propulsion and Power 9 (4),(1993)499-514.

[8] Tishko, J. M., J. P. Drummond, T. Edwards, and A. S. Nejad , Future direction of supersonic combustion research, AIAA Paper (1997)97-1017.

[9] Abbitt, J. D., C. Segal, J. C. McDaniel, R. H. Krauss, R. B. Whitehurst, Experimental supersonic hydrogen combustion employing staged injection behind a rearward-facing step, Journal of Propulsion and Power 9 (3),(1993)472-479.

[10] Riggins, D.W.,McClinton, C. R., Rogers, R. C., Bittner, R. D., Investigation of Scramjet Injection Strategies for HighMach Number Flows, Journal of Propulsion and Power,11(3),(1995)409-418.

[11] Zukoski, E. E. , F. W. Spaid, Secondary injection of gases into a supersonic flow., AIAA Journal ,2 (10),(1999)1689-1696.

[12] Schetz, J. A. ,F. S. Billig , Penetration of gaseous jets injected into a supersonic stream, Journal of Spacecraft and Rockets ,3 (11),(1966) 1658-1665.

[13] Rogers, R. C. , A study of the mixing of hydrogen injected normal to a super-sonic airstream , NASA TN D-6114,(1971).

[14] Rothstein, A. D. ,P. J. Wantuck , A study of normal injection of hydrogen into a heated supersonic flow using Planar Laser-Induced Fluorescence, AIAA Paper (1992)92-3423.

[15] Papamoschou, D. , D. G. Hubbard , Visual observations of supersonic transverse jets, Experiments in Fluids 14,(1993)468-476.

[16] Ben-Yakar et.al. Experimental investigation of flame-holding capability of a transverse hydrogen jet in supersonic cross-ow, Seventh International Symposium on Combustion, The Combustion Institute,(1998b)2173-2180.

[17] Ben-Yakar, A. ,R. K. Hanson , Hypervelocity combustion studies using simultaneous OH-PLIF and schlieren imaging in an expansion tube , AIAA Paper,(1999a)99-2453.

[18] Kyung Moo Kim , Seung Wook Baek , Cho Young Han, Numerical study on supersonic combustion with cavity-based fuel injection,, International Journal of Heat and Mass Transfer ,47 ,(2004)271286.

[19] Kim et.al. "Numerical study on supersonic combustion with cavity-based fuel injection", *International Journal of Heat and Mass Transfer* ,47,(2003)271-286.

[20] Wei Huang,Wei-dong Liu,Shi-binLi,Zhi-xunXia,JunLiu,Zhen-guoWangn, Influences of the turbulence model and the slot width on the transverse slot injection flow field in supersonic flows , Acta Astronautica 73,(2012)19.

[21] J.V. Foa,and G.Rudinger, "Heat addition to a flowing gas", J. aero. Sci., 16,(1949)566-570.

[22] P.M.Stocker, The transients arising from the addition of heat to a gas flow, Mathematical Proceedings of the Cambridge of Philosophical Society, 48,(1952)482-498.

[23] A.Ferri, "Mixing-controlled supersonic combustion", Annual Review of Fluid Mechanics,5,(1973)301-338.

[24] W.H.Heiser, D.T. Pratt, Hypersonic air breathing propulsion, AIAA,(1994)251-257.

[25] E.T.Curran, S.N.B. Murthy, Scramjet Propulsion, *Progress in Astronautics and Aeronautics*, 189, AIAA (2000).

[26] J.M.Seiner, S.M. Dash, D.C. Kenzakowski, "Historical survey on enhanced mixing in scramjet engines", Journal of Propulsion and Power,17(6),(2001)1273-1286.

[27] S.A.Rowan, A. Paull, "Performance of a scramjet combustor with combined normal and tangential fuel injection", *Journal of Propulsion and Power*, 22,(2006)1334-1338.

[28] R.A.Baurle, M.R. Gruber, Study of recessed cavity flow fields for supersonic combustion applications, AIAA Paper (1998)98-0938.

[29] A.Ben-Yakar, R. Hanson, Cavity flameholders for ignition and flame stabilization in scramjets, Review and Experimental Study, AIAA Paper (1998)98-3122.

[30] T.Mathur, M. Gruber, K.Jackson, J.Donbar, W.Donaldson, T.Jackson, F. Billig, "Supersonic combustion experiments with a cavity-based fuel injector", *Journal of Propulsion and Power*,17(6),(2001)1305-1312.

[31] J.H. Kim, Y. Yoon,I.S.Jeung, H. Huh,J.Y.Choi, Numerical study of mixing enhancement by shock waves in model scramjet engine, AIAA Journal, 41,(2003)1074-1080.

[32] Z. A. Rana, B. Thornber, D. Drikakis, Transverse jet injection into a supersonic turbulent cross-flow, Physics of Fluids, 23,(2011) 046-103.

[33] W. Waidmann, F. Alff, M. Bohm, U. Brummund, W. Clauss, M. Oschwald, Experimental investigation of hydrogen combustion process in a supersonic combustion ramjet (SCRAMJET), in: DGLR Jahrbuch,(1994) 629-638.

[34] W. Waidmann, F. Alff, M. Bohm, U. Brummund, W. Clauss, M. Oschwald, Supersonic combustion of hydrogen/air in a scramjet combustion chamber, Space Technology, 15(6),(1995)421-429.

[35] W. Waidmann, U. Brummund, J. Nuding, Experiments investigation of supersonic ramjet combustion (Scramjet), in: 8th International Symposium on transport phenomena in combustion,San Francisco, USA, 1995.

[36] Michael Oevermann, Numerical investigation of turbulent hydrogen combustion in a scramjet using flamelet modeling, *Aerospace Science Technology*, 4,(2000)463-480.

[37] M. Berglund, C. Fureby, LES of supersonic combustion in a scramjet engine model, Proceedings of the Combustion Institute, *Proceedings of the Combustion Institute*, 31,(2007) 2497-2504.

[38] K. Kumaran, V. Babu, Investigation of the effect of chemistry models on the numerical predictions of the supersonic combustion of hydrogen, Combustion and Flame, 156,(2009) 826-841.

[39] Malsur Dharavath, P. Manna, Debasis Chakraborty, Thermochemical exploration of hydrogen combustion in generic scramjet Combustor, *Aerospace Science and Technology* , In press, Available on line December (2011).

[40] J.P. Dussage, P. Dupont, J.F. Debieve, Unsteadiness in shock wave boundary layer interactions with separation, Aerospace Science and Technology, 10,(2006)85-91.

[41] B .Ganapathisubramani, N.T. Clemens, D.S. Dolling, Effect of upstream boundary layer on shock-induced separation, *J. Fluid Mech.*, 585,(2007)369-394.

[42] R.A. Humble, G.E.Elsinga, F. Scarano, B.W. van Oudheusden, Investigation of the instantaneous 3-D flow organization of a shock wave/turbulent boundary layer interaction using tomographic PIV, 37th AIAA Fluid dynamics conference and Exhibit, AIAA-4112, (2007).

[43] J.R .Edwards, Numerical simulations of shock/boundary layer interactions using timedependent modeling techniques: a survey of recent results, *Progress in Aerospace Sciences*, 44,(2008)447-465.

[44] XuXu, XuDajun, CaiGuobio, Optimization design for scramjet and analysis of its operation performance, *Acta Astronautica*, 57,(2005)390-403.

[45] Om Prakash Raj, K. Venkatasubbaiah, A new approach for the design of hypersonic scramjetinlets, *Phys. Fluids*, 24,(2012)086-103.

[46] F.W.Spaid, E.R.Keener,F.C.L.Hui, Experimental Results For a Hypersonic Nozzle/After body FlowField, NASATM-4638(1995).

[47] R. Lederer, W. Kruger, Development as a Key for Hypersonics, *AIAA Paper*,(1993)93-5058.

[48] Lebanon, FLUENT 6.3 User's Guide, FLUENT, I., NH: Fluent Inc.(2006).

[49] D.B. Spalding. Mixing and chemical reaction in steady confinedturbulent flames. In 13th Symp. (Int'l.) on Combustion. The Combustion Institute, (1970).

[50] J.D. Ferguson, D.K. Walters, J.H. Leylek Performance of turbulence models and near-wall treatments in discrete jet film cooling simulations. ASME 43rd International Gas Turbine Aero engine Congress Exhibition, Stockholm, Sweden, United States (1998).

[51] J.D. Ferguson, D.K. Walters, J.H. Leylek Performance of turbulence models and near-wall treatments in discrete jet film cooling simulations. ASME 43rd International Gas Turbine Aero engine Congress Exhibition, Stockholm, Sweden, United States (1998).

[52] Stephen M. Ruffin, Ethiraj Venkatapathy, Earl R. Keener, and Frank W. Spaid, "Hypersonic single expansion ramp nozzle simulations", *Journal of Spacecraft and Rockets*, 29(6),(1992)749-755.

[53] Hirschen, Christian and Glhan, Ali , ,Experimental Study of the Single Expansion Ramp Nozzle Flow Properties and its Interaction with the External Flow, In: Conference Proceedings 1st Gas Air and Space Conference. 1st Gas Air and Space Conference, 2007-09-10 - 2007-09-13, Berlin (Germany). (2007)ISSN 0070-4083.

[54] Christian Hirschen, Ali Glhan, Walter Beck, and Ulrich Henne, Pitot Survey of Exhaust Flow Field of a 2-D Scramjet Nozzle at Mach 6 With Air or Freon and Argon Used for Exhaust Simulation, *Journal of Propulsion and Power*, 24(4),(2008)662-672.

[55] W.J. Monta, Pitot Survey of Exhaust Flow Field of a 2-D Scramjet Nozzle at Mach 6 With Air or Freon and Argon Used for Exhaust Simulation", *NASA* , TM-4361 (1992).

[56] C. Hirschen, A. Gulhan, Influence of heat capacity ratio on pressure and nozzle flow of scramjets, *J. Propul. Power* , 25 ,(2009)303311.

[57] J.P. Li, W.Y. Song, Y. Xing, F.T. Luo, Influences of geometric parameters upon nozzle performances in scramjets, *Chin. J. Aeronaut.*, 21 ,(2008)506511.

[58] V. Thiagarajan, S. Panneerselvam, E. Rathakrishnan, Numerical flow visualization of a single expansion ramp nozzle with hypersonic external flow, *J. Visualization .*, 9 ,(2006)9199.

[59] Hirschen, Christian and Glhan, Ali , Experimental Study of the Single Expansion Ramp Nozzle Flow Properties and its Interaction with the External Flow, In: Conference Proceedings 1st Gas Air and Space Conference. 1st Gas Air and Space Conference, 2007-09-10 - 2007-09-13, Berlin (Germany). (2007)ISSN 0070-4083.

[60] Tetsuo Hiraiwa, Sadatake Tomioka, Shuuichi Ueda, Tohru Mitani, Masahiko Ya-mamoto, and Masashi Matsumoto, Performance variation of scramjet nozzle at various nozzle pressure ratios", *Journal of Propulsion and Power*, 11(3),(1995)403-408.

[61] W. Huang, Z.G. Wang, S.B. Luo, J. Liu, , An overview of research on engine/airframe integration for hypersonic waverider vehicles , *(in Chinese), J. Solid Rocket Technol.*,32,(2009)242248.

[62] Saniovanni J J, Barber T J, Syed S A., Role of hydrogen/air chemistry in nozzle performance for hypersonic propulsion system , *Journal of Propulsion and Power*,9(1),(1993)134-138.

[63] Lee S H, Mitani T., Reactive flow in scramjet external nozzle, *AIAA*,99-0616 ,(1999).

[64] Wei Huang a,n, Zhen-guo Wang a,n, Derek B.Ingham b, LinMab, Mohamed Pourkasha-nian, , Design exploration for a single expansion ramp nozzle (SERN) using data mining, *Acta Astronautica* ,83 ,(2013)1017.

[65] Bardina, J.E., Huang, P.G., Coakley, T.J., Turbulence Modeling Validation, Testing, and Development, *NASA*,Technical Memorandum (1997)110-446.

[66] S. Aso et al., Experimental study on mixing phenomena in supersonic flows with slot injection, AIAA-91-0016,(1991).

[67] Z.A. Rana, B. Thornber, D. Drikakis, On the importance of generating accurate turbulent boundary condition for unsteady simulations, J. Turbulence ,12(35),(2011)139.

[68] C. Segal, The Scramjet Engine Processes and Characteristics, Cambridge University Press, UK, (2009).

[69] F.W. Spaid, E.E. Zukoski, A study of the interaction of gaseous jets from transverse slots with supersonic external flows, AIAA Journal ,6(2),(1968)205212.

[70] McMillin, B. K., Seitzman, J. M., and Hanson, R. K., Comparison of NO and OH Planar Fluorescence Temperature Measurements in Scramjet Model Flow. elds, AIAA Journal, Vol. 32, No. 10,(1994)19451952.

[71] Riggins, D.W.,McClinton, C. R., Rogers, R. C., and Bittner, R. D., Investigation of Scramjet Injection Strategies for HighMach Number Flows, Journal of Propulsion and Power,11(3),(1995)409418.

[72] D.B. Spalding, Mixing and chemical reaction in steady confinedturbulent flames. In 13th Symp. (Int'l.) on Combustion. The Combustion Institute, (1970).

[73] J.D. Ferguson, D.K. Walters, J.H. Leylek, Performance of turbulence models and near-wall treatments in discrete jet film cooling simulations. ASME 43rd International Gas Turbine Aero engine Congress Exhibition, Stockholm, Sweden, United States (1998).